POLITECNICO
DI TORINO
Dipartimento
di Scienza Applicata
e Tecnologia

chimica
fisica
materiali
DiSAT
Dipartimento di Eccellenza

SIOF
Società Italiana
di Ottica e Fotonica
Plasmonica & Nano-Ottica Working group

3rd International School on Plasmonics and Nano-Optics

July 4-7 | Torino, Italy

Politecnico di Torino

https://www.plasmonica.it/2022school/

PLASMONICA 2022

Topics

- Plasmon-enhanced Spectroscopies
- 2D Nano-Optics and Polaritonics
- Spin-orbit coupling phenomena
- Novel materials
- Ultrafast and Non-linear Light-Matter Interactions
- Plasmon Catalysis

International School on Plasmonics and Nano-Optics, Turin 4-7 July 2022 – Final Program

	Monday 4th July	Tuesday 5th July	Wednesday 6th July	Thursday 7th July
9.00-10.45	Registration/ Introduction	**Annamaria Gerardino**	**Lorenzo Marrucci**	*Welcome Coffee*
10.45-11.30	*Coffee Break*	*Coffee Break*	*Coffee Break*	**PLASMONICA 2022 Workshop Opening**
11.30-13.15	**Jaime Gómez Rivas**	**Alfred J. Meixner**	**Bert Hecht**	
13.15-14.15	*Lunch*	*Lunch*	*Lunch*	
14.15-16.00	**Stefanie Gräfe**	**Pietro Gucciardi**	**Giulio Cerullo**	
16.00-16.45	*Coffee Break*	*Coffee Break*	*Coffee Break*	
16.45-17.25	**Selected Talks** *G. Conte* *M. Trevisani*	**Selected Talks** *M. Manoccio* *M. David*	**Selected Talks** *L. Guarneri* *O. Pashina* *G. Ferrando*	
17.25-18.40	**E. Perotti (COMSOL)**	**M. Unger (Bruker)** **M. Hrabovsky (Tescan)**	**17.45 Aperitif & Poster session**	
				Social Dinner

LIST OF LECTURERS

Giulio Cerullo	«Ultrafast processes in plasmonic nanostructures»
Annamaria Gerardino	«How to realize photonic and plasmonic devices? Nanofabrication process design and technology for a challenging task»
Jaime Gómez Rivas	«Collective Plasmonic Resonances»
Stefanie Gräfe	«Plasmon Catalysis»
Pietro Gucciardi	« Advanced nanostructures and substrates for thermophoretic concentration and SERS detection »
Bert Hecht	«How to build plasmonic nanomotors to drive microdrones»
Lorenzo Marrucci	«Spin-orbit optical phenomena»
Alfred J. Meixner	«Plasmonics and Nano-Optics for Chemical Sensing»

LIST OF TUTORIALS

Elisabetta Perotti	«Plasmonics and Modeling in COMSOL Multiphysics»
Milos Hrabovsky	«Fabrication of Plasmonic nanostructures via Nanoprototyping applications using FIBSEM systems»
Miriam Unger	«2D Material Characterization Using Nanoscale IR Spectroscopy and Imaging with a Versatile Broadband IR Laser Source»

LIST OF SELECTED SPEAKERS

Gloria Conte	«Bound states in the continuum in dielectric metasurfaces»
Mauro David	«Surface-enhancement of ultra-broadband mid-IR plasmonic waveguides for liquid spectroscopy applications»
Giulio Ferrando	«Large-scale metasurfaces for plasmon enhanced photobleaching of dye molecules»
Ludovica Guarneri	« Excitonic scattering in atomically-thin optical elements»
Mariachiara Manoccio	«3D Helix-based Metamaterial Arrays for Femtomolar Biodetection»
Olesia Pashina	«Thermooptical conversion of SHG radiation from semiconductor nanodimers»
Mirko Trevisani	«Coherent photon sources based on 2D Al periodic nanostructures»

List of posters

Wednesday 6th July Poster session		
1	S. Balestrieri	Plasmonic Nanodevice to induce strong EM field gradient
2	L. Bonatti	In-silico design of graphene plasmonic hot-spots
3	G. Di Maio	Gold nanocubes two dimensional mo nolayers: preparation and characterization of versatile plasmonic substrate
4	G. Ferrando	Microfabricated SiN membrane applied as a free-standing waveguide for refractive index sensing
5	B. Hinkov	A mid-infrared lab-on-a-chip for real-time reaction monitoring of liquids
6	A. Intze	Mid-Infrared Nanospectroscopy of Misfolded Protein Aggregates
7	Y. Luan	Near-Unity Third-Harmonic Circular Dichroism in Silicon Chiral Metasurfaces
8	R.Magrin Maffei	Electrical Modulation of the Optical Response of an Al-doped ZnO Thin Film
9	A. Mohan	Magnetically co-doped Indium Tin Oxide nanoparticles (ITO-NPs) for magnetoplasmonic refractometric sensing
10	L. Ramò	Local optical properties of CVD-grown ML-WS2 flakes on an ultra-dense plasmonic array of Au NPs
11	S. Sotgiu	Raman scattering with near infrared excitation selectively resonant with the indirect bandgap of bulk MoSe2
12	M.E. Temperini	Infrared nanospectroscopy study of light-sensitive proteins with a plasmonic probe
13	D. Urban	Light-triggered reversible deformations of a polymeric substrate in arbitrary directions
14	R. Büchner	Plasmon-Induced Circular Dichroism of Gold Nanoparticles of Different Shapes

15	M. Dieperink	Determining the optical properties of Au nanorods using the metal nanoparticle boundary element method
16	S. Ehtesabi	Plasmon-driven Reactivity and Selectivity on Metal Nanoparticles Assessed by Quantum Chemical Simulations
17	Q. Nguyen	Bottom-up and top-down synthesis of Au@AZO core@shell nanomaterials
18	D. Ryabov	Thermo-optical bistability in single semiconductor super-cavity
19	F. Scalerandi	Charge transfer in hybrid metal-semiconductor systems at a single NP level and correlation to morphology
20	A. Verneuil	Nonlinear optical sensing in arrays of plasmonic nanoparticles
21	S. Thakur	Shaping ZnO nanoparticles: Effect of nanoparticle morphology on caffeine degradation
22	T. Hoekstra	Actively tunable hybrid-2D angle-sensing photodetectors

Organization

- Alessandro Belardini –SAPIENZA Università di Roma
- Alessandro Chiadò –Politecnico di Torino
- Emiliano Descrovi –Politecnico di Torino
- Ambra Giannetti –CNR – Istituto di Fisica Applicata IFAC
- Fabrizio Giorgis –Politecnico di Torino
- Chiara Novara –Politecnico di Torino
- Paola Rivolo –Politecnico di Torino

Scientific Committee

- Paolo Biagioni –Politecnico di Milano
- Michele Celebrano –Politecnico di Milano
- Stefania D'Agostino –CNR Nanotec
- Enzo Di Fabrizio –Politecnico di Torino
- Carlo Forestiere –Università degli Studi di Napoli Federico II
- Maria Caterina Giordano –Università di Genova
- Michele Ortolani –SAPIENZA Università di Roma

School Location

The Politecnico di Torino main campus is a large complex of buildings in Corso Duca degli Abruzzi. It was opened in November 1958, after the former Industrial Museum was completely destroyed during World War II. The construction of the new Cittadella Politecnica in Corso Castelfidardo began in 1997 when Politecnico di Torino acquired the former Officine Grandi Riparazioni. The Cittadella is a single integrated complex of buildings of high architectural and urban value whose spaces are used by companies and management services, University and individual citizens

How to reach Politecnico di Torino

The easiest way to reach the conference location is by entering the Cittadella Politecnica of the Polytechnic University of Turin from the parking entrance located in Corso Castelfidardo 42bis, underneath the south bridge. It is ten minutes from the Porta Susa train station.

In alternative, you can take the Metro line from either Porta Susa or Porta Nuova train stations and get off at the "Vinzaglio" stop. Inside the Politecnico you will find signs carrying the Plasmonica 2022 logo pointing to the conference rooms (Classrooms P). Support staff will eventually assist you to reach the conference site.

Selected Talks

Bound states in the continuum in dielectric metasurfaces

Gloria Conte[1,2], *Simone Zanotto*[2], *Laurent Belleries*[3], *Amadeu Griol*[3], *Daniel Navarro-Urrios*[4],
Alessandro Tredicucci[1,2], *Alejandro Martínez*[3] and *Alessandro Pitanti*[2]
[1]*Dipartimento di Fisica, Università di Pisa, Italy, gloria.conte@phd.unipi.it*
[2]*NEST Lab., CNR - Istituto di Nanoscienze and Scuola Normale Superiore, Pisa, Italy*
[3]*Nanophotonics Technology Center, Universitat Politècnica de València, Spain*
[4]*MIND-IN2UB, Departament d'Electrònica, Facultat de Física, Universitat de Barcelona, Spain*

Bound states in the continuum (BICs) [1] are modes that reside inside the continuum, but remain perfectly localized without radiating energy away. BICs are a general wave phenomenon that has been identified even in optical systems [2], including photonic crystal slabs [3] and metasurfaces [4]. BICs result from interference effects and therefore can be found interrogating the system at precise frequencies and wavevectors. While pure BICs have infinite Q factors and are therefore invisible to external probes, in close proximity to them narrow resonances can be found and experimentally investigated (quasi-BICs). Signature of the presence of the BIC is the line-narrowing effect moving from a quasi-BIC towards a pure BIC. A simulation depicting this effects is shown in Figs. 1(a) and 1(b) for a Si metasurface.

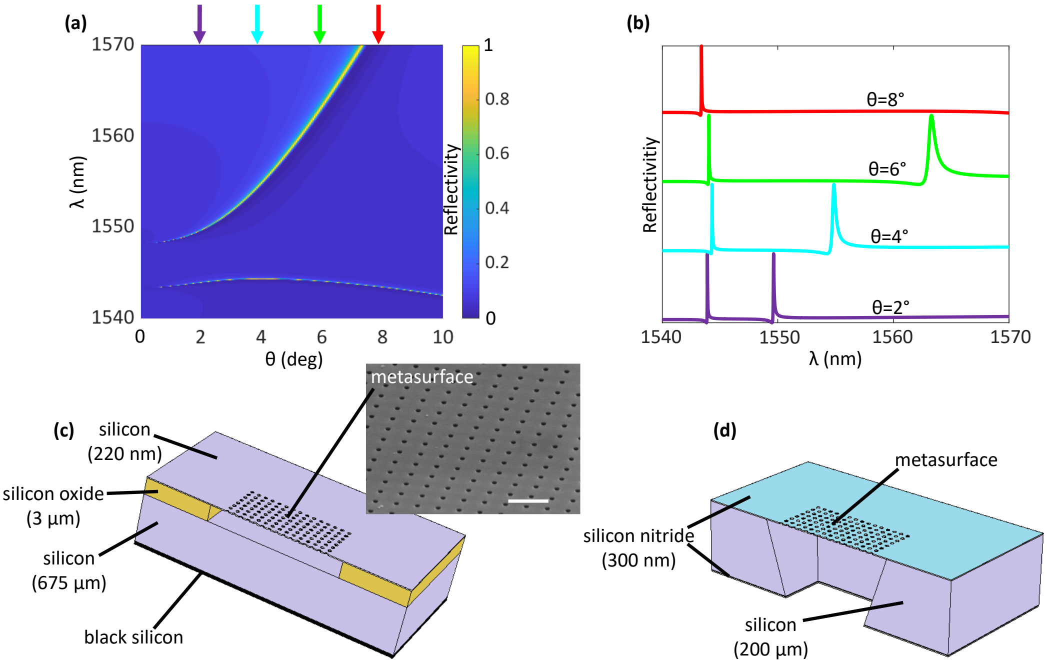

Figure 1: (a) Reflectivity map of a completely suspended silicon metasurface (see panel c). Two modes appear with a line narrowing towards $\theta = 0°$, see cross-sections in (b). Sketch of a silicon (c) and a silicon nitride (d) metasurface device. In the inset of panel c a SEM image of one Si metasurface is shown [5]; the white scale bar is 1 μm.

We experimentally investigated BICs in mechanically compliant devices, namely all suspended Si and Si_3N_4 metasurfaces. While the former shows non-trivial coupling between the BIC resonance, substrate Fabry-Perot fringes and mechanical action of the membrane (see Fig. 1(c)) [5], the latter (see Fig. 1(d)) can be a platform for the investigation of the pure optomechanical coupling between BICs and membrane modes.

References

[1] C. W. Hsu, B. Zhen, A. D. Stone, J. D. Joannopoulos and M. Soliačić, Nat. Rev. Mater. **1**, 16048 (2016).
[2] Y. Plotnik, O. Peleg, F. Dreisow, M. Heinrich, S. Nolte, A. Szameit and M. Segev, Phys. Rev. Lett.**107**, 183901 (2011).
[3] C. W. Hsu, B. Zhen, J. Lee, S. Chua, S. G. Johnson, J. D. Joannopoulos and M. Soliačić, Nat. Rev. Mater. **1**, 16048 (2016).
[4] T. C. W. Tan, E. Plum and R. Singh, Adv. Opt. Mater. **8**, 1901572 (2020).
[5] S. Zanotto, G. Conte, L. C. Belleries, A. Griol, D. Navarro-Urrios, A. Tredicucci, A. Martínez and A. Pitanti, Phys. Rev. Appl. **17**, 044033 (2022).

Coherent photon sources based on 2D Al periodic nanostructures

Mirko Trevisani[1], *Diego Piccotti*[1], *Giuseppe Pirruccio*[2], *Tiziana Cesca*[1], *Giovanni Mattei*[1]
[1]*University of Padova, Padova, Italy, mirko.trevisani@phd.unipd.it*
[2]*Universidad Nacional Autonoma de México, Mexico City, Mexico*

Keywords: Nanolaser, Plasmonics, Nanophotonics.

Nowadays, the request of highly coherent and miniaturized laser sources has been increased according to the fabrication of faster and smaller devices. Plasmonic nanolasers are one of the most innovative types of laser, thanks to their low lasing threshold, high directionality and small device volume. The combination of all those peculiar properties makes them attractive for several applications ranging from biosensing, to quantum information. [1] These devices are based on periodic array of plasmonic nanoparticles that shows hybrid resonant modes, called "Surface Lattice Resonances" (SLR), which act as optical feedback for lasing emission when the structure is coupled to a quantum emitter. Depending on the geometry, dimension and shape of nanoparticle and surrounding, the optical and lasing properties can be easily tailored. [2–4]

In this work we used an hexagonal array of Aluminium nanocones with lattice constant $a = 475nm$ and particle height and diameter of $h = 150nm$, $d = 150nm$, respectively. The array was fabricated by EBL on a quartz substrate and on top, a layer of $300nm$ of PMMA containing an organic dye was deposited via spin coating. Figure 1(a) displays the optical band structures of the periodic array, performed by angle-resolved transmission measurements along the high-symmetry directions (ΓM). Finite Element Method (FEM) simulation with the software COMSOL Multiphysics were used to investigate field distribution and the modes' properties. According to the dye optical properties, the resonant energy exchange with SLR modes occurs at the Γ point, so too the lasing emission. Figure 1(b)-(c) show the lasing emission peak at about $600nm$ when a 18 ps-pulsed laser at $532nm$ with TE polarization and incidence angle $\theta = 18.1°$ is used with fluence F above $0.51mJ/cm^2$. Angular measurement has been performed confirming the high directionality of the peak emission with a value of 1.2° around the Γ point comparable to the angular resolution of our optical setup. The FWHM of the emission peak at 0° is $0.7nm$, thus demonstrating a high degree of monochromaticity of the laser beam. The remarkable temporal coherence of the emission (above $0.5mm$) has been confirmed by a Michelson-Morley interferometer.

The reported results prove that these types of device are very good candidates for the development of nanolaser with increased performance and decreased dimensions.

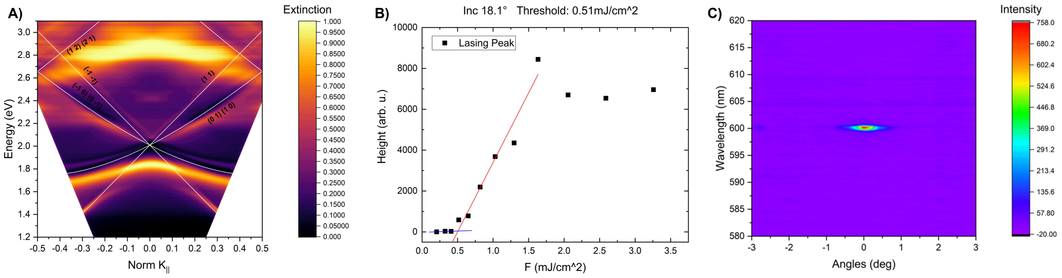

Figure 1: **A)** Extinction map of Al nanocones array taken in TE mode along the direction $\Gamma - M$ with the Rayleigh anomalies superimposed (black lines) and labelled with the corresponding Miller indexes. **B)** Peak height of the emission at $600nm$ as a function of the pump fluence (threshold). **C)** Angular emission map excited with a fluence of $0.8mJ/cm^2$ (above lasing threshold) and incidence angle $\theta = 18.1°$.

References

[1] V. G. Kravets, A. V. Kabashin, W. L. Barnes, and A. N. Grigorenko, Chem. Rev. 118, 5912-5951 (2018).
[2] A. Yang, T. B. Hoang, M. Dridi, C. Deeb, M. H. Mikkelsen, G. C. Schatz, and T. W. Odom, Nat Commun 6, (2015).
[3] R. Guo, M. Necada, T. K. Hakala, A. I. Väkeväinen, and P. Törmä, Phys. Rev. Lett. 122, (2019).
[4] X. G. Juarez, R. Li, J. Guan, T. Reese, R. D. Schaller, and T. W. Odom, ACS Photonics 9, 52-58 (2022).

3D Helix-based Metamaterial Arrays for Femtomolar Biodetection

Mariachiara Manoccio[1,], Marco Esposito[1] , Elisabetta Primiceri[1] , Vittorianna Tasco[1], Massimo Cuscunà[1] ,
and Adriana Passaseo[1]*

1 CNR NANOTEC Institute of Nanotechnology, Via Monteroni, 73100 Lecce, Italy

e-mail: mariachiara.manoccio@nanotec.cnr.it

Keywords: Plasmonics, Biosensing, Chirality

The continuous progress in the nanostructure manufacturing broadened several application areas for nanophotonics. In such a frame, realizing chiral nanostructures, though technologically challenging, can enable novel degrees of freedom in optical engineering through polarization control. Chiral engineering can be applied at a material level with the definition of specific compositional layouts, or at a geometrical level, with the spatial arrangement in the three dimensions, given the availability of suitable technology.
In this contribution we will show our activities on the multiple level engineering of chiral objects at the nanoscale, by the exploitation of focused ion beam technique. In particular, we studied new strategies for shaping metal-dielectric core-shell systems, either exploiting directly the liquid ion source of the system in combination with a metal organic precursor, or by post-growth conformal coating with polymeric layers.
We also investigated the diffractive coupling regime among multiple elements, along the in-plane and out of-plane directions, to achieve control over the circular dichroism (CD) signature through 3D lattice parameters.
The results of the study are applied to innovative sensing concepts based on chiral platforms based on circular dichroism measurements, for highly sensitive and selective biomolecular detection, in different environments, such as biological fluids.

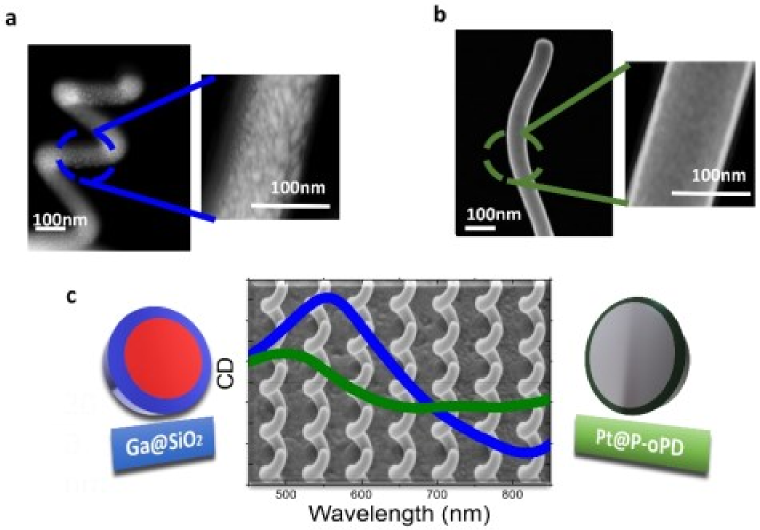

Figure 1. (a) SEM image of nano-helix array. The magnification of a SEM image area (b) displays the geometrical parameters of helix the array: the vertical period (VP), the wire diameter (WD) 120nm, the external diameter (ED) 310nm, and the lateral period (LP) 500nm.

References

[1]Esposito, M.; Manoccio, M.; Leo, A.; Cuscunà, M.; Sun, Y.; Ageev, E.; Zuev, D.; Benedetti, A.; Tarantini, I.; Passaseo, A.; et al. 3D Chiral MetaCrystals. *Adv. Funct. Mater.* **2021**, *n/a*, 2109258, doi:https://doi.org/10.1002/adfm.202109258.
[2] Manoccio, M.; Esposito, M.; Primiceri, E.; Leo, A.; Tasco, V.; Cuscunà, M.; Zuev, D.; Sun, Y.; Maruccio, G.; Romano, A.; et al. Femtomolar Biodetection by a Compact Core–Shell 3D Chiral Metamaterial. *Nano Lett.* **2021**, doi:10.1021/acs.nanolett.1c01791.
[3]Cuscunà, M.; Manoccio, M.; Esposito, M.; Scuderi, M.; Nicotra, G.; Tarantini, I.; Melcarne, A.; Tasco, V.; Losurdo, M.; Passaseo, A. Gallium chiral nanoshaping for circular polarization handling. *Mater. Horizons* **2021**, *8*, 187–196, doi:10.1039/D0MH01078B.

Surface-enhancement of ultra-broadband mid-IR plasmonic waveguides for liquid spectroscopy applications

Mauro David[1*], Masiar Sistani[1], Felix Frank[2], Ismael C. Doganlar[1], Daniele Nazzari[1], Alicja Dabrowska[2]
Georg Marschick[1], Elena Arigliani[1], Hermann Detz[1,3], Bernhard Lendl[3], Walter M. Weber[1], Gottfried Strasser[1], and Borislav Hinkov[1,*]
[1] *Institute of Solid Stated Electronics, TU Wien, 1040 Vienna, Austria*
[2]*Institute of Chemical Technologies and Analytics, TU Wien, 1060 Vienna, Austria*
[3]*CEITEC, Brno University of Technology, Brno, Czech Republic*
**mauro.david@tuwien.ac.at; borislav.hinkov@tuwien.ac.at*

Keywords: Sensors and Biosensors, Spectroscopy, Devices and Applications.

Mid-infrared (mid-IR) spectroscopy is a powerful tool for probing the fingerprint absorptions of molecules in gas and liquid phase, particularly important for the chemical and biomedical fields. Thanks to the development of high-performance quantum cascade lasers (QCLs) and detectors (QCDs), new analytical methods can be developed to enable a new class of miniaturized sensors. While allowing to penetrate thicker layers of the liquid analyte through powerful QCLs, the typical experimental setups are still rather big and bulky[1]. Thus, the next generation of compact sensors needs to implement novel integration concepts. Previous work demonstrated mid-IR plasmonics as a suitable concept for monolithic photonic integrated circuits (PICs) [2], including for liquid sensing. Based on this approach, we present in this work the realization of the next generation of highly-sensitive plasmon-based mid-IR sensors. Our experiments are conducted on ultra-broadband Ge/Au semiconductor-loaded surface plasmon polariton (SLSPP) waveguides [3]. We present in this work the implementation of two novel concepts, which lead to an enhancement of the sample surface of the Ge-based SLSPP waveguides, enabling their use in a much wider range of applications. The first experiment exploits the surface-passivation based on high-quality atomic layer deposition (ALD) coatings, deposited on ultra-broadband Ge/Au-based long-wave infrared plasmonic waveguides [3] (see Fig. 1(a)). As shown in Fig. 1(b), various additional materials can be used for that purpose and protect the Ge surface from water, when submerging the whole chip into the liquid. In the second experiment we functionalize such waveguides by covering them with suitable mesoporous membranes like, e.g. Titania (Fig. 1(a)). As sketched in Fig. 1(c), this yields an enrichment of the analyte in a liquid close to the sensitive plasmonic surface, significantly increasing the plasmonic sensor limit of detection by more than two order of magnitude.

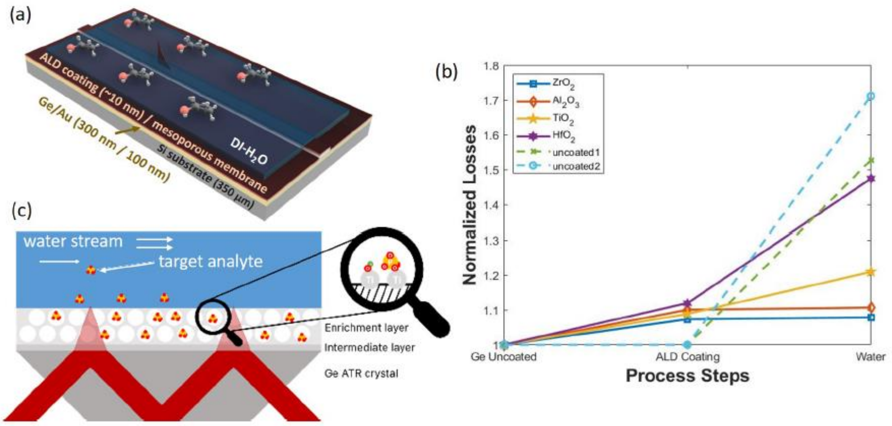

Figure 1: (a) Sketch of a typical Ge/Au SLSPP waveguide structure including ALD coating when submerged into DI-H2O. (b) Characterization results after the submersion experiment. (c) Sketch of a mesoporous membrane coated Ge surface submerged into a liquid analyte. The enrichment of the molecule under investigation close to the sample surface is indicated.

References

[1] A. Schwaighofer, M.R. Alcaráz, C. Araman, H. Goicoechea, B. Lendl, Sci Rep 6 (2016) 33556.

[2] B. Schwarz, P. Reininger, D. Ristanić, H. Detz, A.M. Andrews, W. Schrenk, G. Strasser, Nature Communications 5 (2014) 4085.

[3] M. David, A. Dabrowska, M. Sistani, I.C. Doganlar, E. Hinkelmann, H. Detz, W.M. Weber, B. Lendl, G. Strasser, B. Hinkov, Opt. Express 29 (2021) 43567.

Excitonic light scattering in atomically-thin optical elements

Ludovica Guarneri[1], Qitong Li[2], Jung-Hwan Song[2], Mark Brongersma[2], and Jorik van de Groep[1]
[1] Institute of Physics, University of Amsterdam, Amsterdam, The Netherlands, l.guarneri@uva.nl
[2] Geballe Laboratory for Advanced Materials, Stanford University, Stanford, USA

The interest in monolayers transition metal dichalcogenides (TMDC) stems from the combination of their two-dimensional structure together with the remarkably strong exciton resonances they exhibit in the visible spectral range. Quantum confinement and reduced dielectric screening enable tightly bound excitons that dominate the optical spectra of these atomically thin semiconductors – even at room temperature. Leveraging these remarkable excitonic properties in conjunction with smart cavity engineering has recently led to unprecedent results, namely near unity light absorption [1] and a large excitonic reflectivity up to 85% [2] with a single layer of atoms at cryogenic conditions. In addition to strong light-matter interactions, these geometry-independent resonances are also highly tunable in the visible spectral range. This has resulted in the first demonstration of large-area and tunable flat optics at ambient conditions, albeit with very low efficiency [3]. To fully exploit exciton resonances in tunable flat optics, it is essential to obtain a detailed understanding of the fundamental efficiency limit of atomically-thin elements and the role of the exciton therein.

Here, we study the direct link between the exciton properties and the optical efficiency of atomically-thin optical elements using temperature-dependent optical experiments. We pattern large-area and high-quality exfoliated monolayer WS_2 into an atomically-thin zone plate lens (Fig. 1a) and diffraction grating (Fig. 1b) using electron-beam lithography and reactive-ion etching. Using a custom-built imaging system, we carefully analyze the optical efficiency spectra across a portion of the visible spectral range (570 – 670 nm) as a function of temperature to explore the role of the exciton decay rates in the optical efficiency.

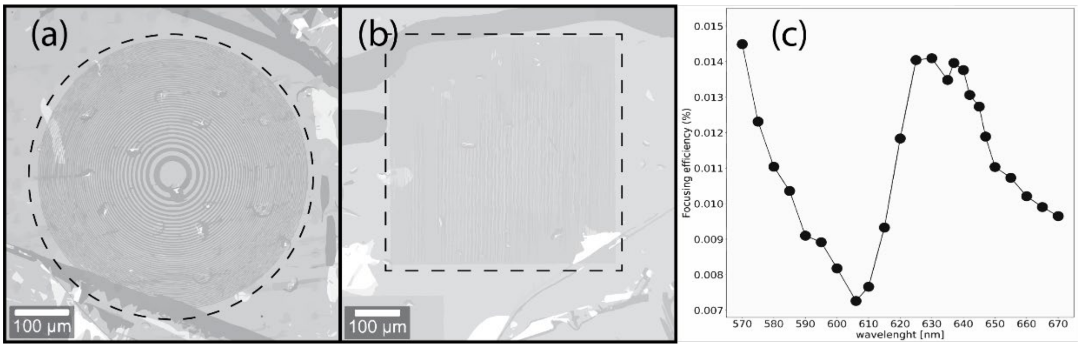

Figure 1: *500 μm diameter zone plate lens with f ~ 1 mm **(a)** and 500×500 μm² diffraction grating with 1.3 μm period **(b)** directly carved out of a monolayer WS₂ on sapphire. **(c)** Experimentally measured focusing efficiency spectrum of the zone plate lens at room temperature.*

At room temperature the focusing efficiency spectrum (Fig. 1c) of the of 500 μm diameter zone-plate lens, yields a strongly asymmetric line shape. This shape mirrors the optical susceptibility of the material, dictated by the presence of the exciton resonance superimposed onto a nearly linear background [3]. Despite the clear exciton fingerprint on its line shape, the focusing efficiency of the lens remains quite low at ambient condition. To explore the fundamental efficiency limit of excitonic light scattering and the dependence of the lens efficiency on the exciton dynamics, we cool the sample to cryogenic temperatures (<10K). In this regime, phonons are suppressed and we expect the exciton to become radiation-limited as a result of low non-radiative and dephasing rates. By analyzing the efficiency spectra, we directly relate the quantum mechanical properties of the exciton to the efficiency limit of atomically-thin classical optical elements.

References

[1] I. Epstein et al., Nano Letters 20, 3545−3552 (2020).
[2] G. Scuri et al., Physical Review Letters 120, 037402 (2018).
[3] J. Van de Groep et al., Nature Photonics 14, 426–430 (2020).

Thermooptical conversion of SHG radiation from semiconductor nanodimers

Olesia Pashina[1], *Kristina Frizyuk*[1], *George Zograf*[1], *Mihail Petrov*[1]
[1]*School of Physics and Engineering, ITMO University, St. Petersburg, Russia, 197101*
olesiya.pashina@metalab.ifmo.ru

In recent years, thermooptical effects arising from laser excitation of resonant nanostructures and accompanying heating have opened up wide possibilities for light control at the nanoscale [1]. These processes are associated with pronounced dependence of the material refractive index on the temperature.

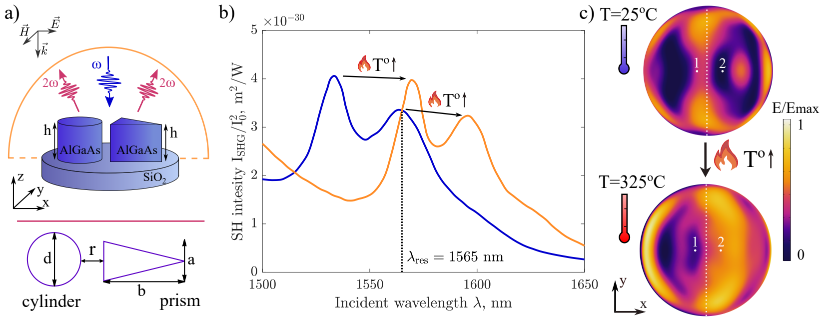

Figure 1: Thermally-induced modification of SHG from cylinder-prism nanodimer. a) Schematic view of the structure, where $h = 400\,\text{nm}$, $d = 386\,\text{nm}$, $a = 350\,\text{nm}$, $b = 460\,\text{nm}$, $r = 200\,\text{nm}$. b) Normilized SHG intensity I_{SHG}/I_0^2 at 25°C (blue) and 325°C (orange). c) SHG radiation collected on the upper hemisphere at fundamental wavelength of 1565 nm at room and elevated temperature. Points 1 and 2 stand for switched dominant contributions of the SHG.

In this work, we theoretically study the phenomenon of photothermal conversion of the second harmonic generation (SHG) radiation pattern from a semiconductor nanostructure [2]. In the proposed geometry (Fig. 1a), a pulsed near-IR laser excites SH radiation from the AlGaAs dimer, while its temperature changes from room (25°C) to elevated one (325°C) due to optical heating by CW visible laser. Upon heating, a spectral shift of the resonant spectral lines occurs due to the described thermorefractive effect, which causes rearrangement of the SH far-field radiation patterns. For more significant reshaping we chose a cylindrical-prismatic dimer that demonstrates a two-peak resonant spectral dependence of the second harmonic near wavelengths of 1500-1650 nm (Fig. 1b). Increasing the temperature results into switching between these resonant peaks separated by a spectral gap of 50 nm. While the long-wavelength SHG resonance corresponds to a wavelength of 1565 nm at room temperature, the short-wavelength peak passes to this wavelength at elevated temperature. This spectral shift is accompanied by a strong change in the shape of the SH far field due to different responses of the cylindrical and prism structures, which contribute to the long-wavelength and short-wavelength peaks. For the two most dominant directions of restructuring, the ratio of SH intensities $I|_{325^oC} \,/\, I|_{25^oC} = 0.5$ and $I|_{325^oC} \,/\, I|_{25^oC} = 23.7$ for points 1 and 2, respectively, during the transition from room temperature to elevated one (Fig. 1c). In this case, the average second-harmonic generation amplitude for different directions can be considered approximately the same for two temperature regimes of the nanodimer, in contrast to a single nanoresonator, which allows a significant rearrangement of the radiation pattern only in conjunction with a sharp decrease in intensity [3]. This effect is achieved precisely due to the dimeric design of the nanostructure, which allows the close location of two resonant SH peaks that can thermally transform into each other.

Thus, in this work, we have proposed an approach to manipulating the directivity of SH radiation due to the thermooptical switching of resonant optical states in the dimeric resonant nanostructure without the significant loss in the SHG value. We believe that our results will pave the way for near-IR thermally-tunable nanoscale optical devices.

References

[1] Zhang, Tianyue, et al. "Anapole mediated giant photothermal nonlinearity in nanostructured silicon." Nature communications 11.1 (2020): 1-9.

[2] Pashina, Olesia, et al. "Thermo-optical reshaping of second-harmonic emission from dimer all-dielectric nanoresonators." Optics Letters 47.8 (2022): 1992-1995.

[3] Pashina, Olesia, et al. "Thermally induced reshaping of second harmonic radiation patterns from resonant semiconductor nanostructures." AIP Conference Proceedings. Vol. 2300. No. 1. AIP Publishing LLC, 2020.

Large-scale metasurfaces for plasmon enhanced photobleaching of dye molecules

Giulio Ferrando[1], Matteo Barelli[1], Maria Caterina Giordano[1], Francesco Buatier de Mongeot[1,*]

[1] *Dipartimento di Fisica, Università di Genova, Via Dodecaneso 33, I-16146 Genova, Italy, *email:buatier@fisica.unige.it*

Keywords: metamaterials, devices and applications, sensor and biosensors

Light harvesting platforms and technologies are necessary in view of the compelling energy and environmental global challenges. Among the viable solutions plasmonic nanoantennas can be very attractive due to their capability to strongly confine electromagnetic fields at the nanoscale, and to enhance light scattering. Notably these peculiar properties can be exploited in photochemical processes [1] with a promising application in waste water treatment and energy storage (exploiting a water splitting process). However, for this kind of applications it is crucial to develop fabrication techniques that are usable over large-areas. Specifically in this work self-organized plasmonic nano-arrays are homogeneously fabricated over macroscopic areas (cm^2) by combining the defocused ion beam irradiation [2] and the physical deposition at glancing angles. In this way tilted Au nanostripes arrays with controlled cross section are formed in a single maskless step over large areas. The nanostripes support Localized Surface Plasmon Resonances (LSPR) [3,4] which can be tuned over a broad range of the Visible and Near-Infrared spectrum by varying the deposition's conditions.

As a demonstration of the surface's functionalization, we test the plasmonic efficiency of these templates into a prototypal photochemical reaction: the photobleaching of the Methylene Blue (MB). We investigate this effect by exciting the system with a monochromatic light source, useful to study in a quantitative way the interaction between the LSPR and the photobleaching of the molecules [5]. We observed a strong increase of the MB's photobleaching when the LSPR is tuned in resonance with the maximum optical absorption of the molecule. This observation highlight the crucial role of the self-organized plasmonic arrays to promote photon harvesting in photochemical processes and energy conversion.

These results pave the way to the optimization of the self-organized plasmonic templates for applications such as waste water treatment by tuning the plasmonic mode in resonance to the absorption of the target molecule. Additionally, applications can be developed in the broader context of nanophotonics, solar energy harvesting, and sensing.

References

[1] Tagliabue, G. *et al.* Quantifying the role of surface plasmon excitation and hot carrier transport in plasmonic devices. *Nat. Commun.* **9**, (2018).

[2] Giordano, M. C. et al. Anisotropic Nanoscale Wrinkling in Solid-State Substrates. *Adv. Mater.* **30**, 1–8 (2018).

[3] Barelli, M., et. al. Color routing via cross-polarized detuned plasmonic nanoantennas in large-area metasurfaces. *Nano Lett*. 20, 6, (2020).

[4] Giordano, M. C., et al. Self-organized nanorod arrays for large-area surface-enhanced infrared absorption. *ACS Appl. Mater. Interfaces*, 12, 9, 11155, (2020).

[5] Barelli, M., et al.. Wavelength-Dependent Plasmonic Photobleaching of Dye Molecules by Large-Area Au Nanostripe Arrays. *ACS Appl. Nano Mater.* **5**, 3470–3479 (2022).

Posters

Plasmonic Nanodevice to induce strong EM field gradient

Sergio Balestrieri[1, 2], Gianluigi Zito[2], Giuseppe Coppola[2], Mario Iodice[2]
[1]*Dipartimento di Fisica, Università di Napoli Federico II, Napoli, Italia, sergio.balestrieri@na.isasi.cnr.it*
[2]*Istituto Scienze Applicate e Sistemi Intelligenti, Consiglio Nazionale Delle Ricerche, Napoli, Italia*

Optical forces are generated using electromagnetic field gradients and have proven to be a powerful tool for manipulating micro- and nano-objects [1].

An effective way to generate such gradients is to use the phenomenon of surface plasmonics, that is the amplification of the electromagnetic field due to the resonant interaction between a light beam and an interface between a dielectric and a metallic material [2]. By appropriately designing such plasmonic structures, it is possible to engineer the electromagnetic field distribution for effective manipulation of nano-objects. Thanks to these characteristics, plasmonic structures have many applications, especially in the medical and biological fields [3]. Moreover, in the last few years a line of research has developed in the aerospace sector aimed at designing plasmonic structures useful for generating optical propulsion for micro/nanosatellites. In this context, a very interesting structure is the one proposed by Rovey's group at the University of Illinois [4,5], in which two gold rectangular trapezoids are separated by a gap and placed on a glass substrate. When light illuminates this structure, the electromagnetic field resulting from plasmonic effects (in particular, from the combination of Localized Surface Plasmon and Surface Plasmon Polaritons) is such as to generate forces capable of ejecting nanoparticles (propellant) and thus inducing propulsion. In addition, the geometry of these structures allows the organization of elementary cells in an array configuration, i.e., to replicate them in a serial manner in order to amplify the force and obtain intensities suitable for the displacement of macroscopic objects. The array configuration, however, involves a spatial distribution of the force that is not optimal for maximising propulsion performance. In fact, in order to obtain effective ejection, it is necessary to induce a strong initial boost to the nanoparticles.

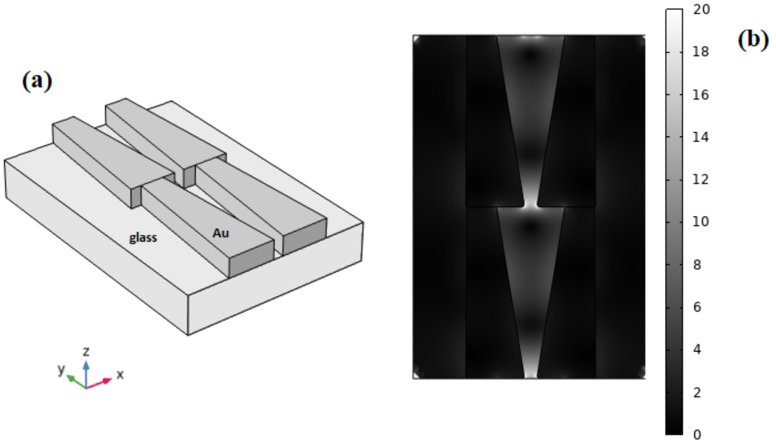

Figure 1: (a) a sketch of the gold scalene trapezoids structure with a glass substrate in array configuration. (b) 2D plot of electric field amplitude at wavelength 830nm in a scalene trapezoids structures.

Therefore, we will discuss a new type of plasmonic structure that overcomes the above limitations. In particular, the proposed system consists of two gold scalene trapezoids separated by a variable gap and placed on a glass substrate. The generated asymmetric field distribution will be analysed as a function of the geometrical parameters of the structure and compared with field distributions generated by structures reported in the literature. The field distribution generated by linear and circular array configurations will also be described. Finally, the procedure to identify the optimal values for the design of an array structure that maximises the force and velocity output parameters for space applications will be illustrated.

References

[1] L.Novothny and B.Hecht, Principles of Nano-Optics, I ed. New York: Cambridge University Press (2006)
[2] Stefan A. Maier, Plasmonics: Fundamentals and Application, I ed. Springer (2007)
[3] A.S. Shalin, S.V. Suckhov, Plasmonics Nanostructures as Accelerators for Nanoparticle: Optical Nanocannon, Plasmonics,8 625-629(2013)
[4] J.L. Rovey, P.D. Fritz, C. Hu, M.S. Glascock and X. Yang, Plasmonic Force Space Propulsion, Journal of Spacecraft and Rockets, 52(4), 1163-1168 (2015)

In-silico design of graphene plasmonic hot-spots

L. Bonatti [*], L. Nicoli [*], T. Giovannini [*], C. Cappelli [*]
[*] Scuola Normale Superiore, Pisa, Italy
luca.bonatti@sns.it

Plasmons are able to confine light down to the nanometer scale and, in turn, to produce an enhancement of the electric field under the effect of an external electromagnetic radiation.[1]
Single molecule detection becomes possible when huge enhancements arise in very precise region of space (i.e. hot spots).[2] Such a confinement is usually obtained by exploiting specific geometrical arrangements of plasmonic substrates, like metal nanoparticles (MNPs).[2]
However, such behavior has not been confirmed for graphene nanostructures, although graphene shows extraordinary optical properties due to the formation of highly localized surface plasmons.[3] In fact, pristine graphene has been used as a substrate for the so-called Graphene Enhancement Raman Scattering (GERS), but the measured enhancement in the molecular Raman signal is orders of magnitude lower than for MNPs.[4]
Therefore, the use of graphene as plasmonic substrate for single molecule detection is being hampered by its low enhancement factors.

In this contribution, we propose a computationally driven design of geometrical arrangements, specifically engineered to maximize the field enhancement in graphene-based nanostructures. Our model is based on a fully atomistic approach that we have recently developed.[5,6]
In particular, we focus on enhancements effects arising close to edge defects and grain boundaries in polycristalline graphene (PCG). Also, we consider geometries inspired by nanocavities allowing single molecule detection on metal substrates.[1]
In all test cases, enhancement factors are comparable to noble metal substrates due to the creation of localized nanocavities, thus potentially paving the way for single molecule detection from graphene-based substrates.

1. Maier, S. A. (2007), Plasmonics: fundamentals and applications, Springer
2. Langer, J. *et al.*, *Acs Nano*, **2019**, 14(1), 28-117
3. Grigorenko, A. N. *et al.*, *Nat. Photonics*, **2012**, 6(11), 749-758
4. Ling, X. *et al.*, *Nano Lett.*, **2010**, 10(2), 553-561
5. Giovannini, T. *et al.*, *Nanoscale*, **2019**, 11(13), 6004-6015
6. Giovannini, T., Bonatti, L., *et al.*, *J. Phys. Chem. Lett.*, **2020**, 11(18), 7595-7602

This work has received funding from the European Research Council (ERC) under the European Union’s Horizon 2020 research and innovation program (grant agreement No. 818064).

Gold nanocubes two-dimensional monolayers: preparation and characterization of versatile plasmonic substrates

Giuseppe Di Maio[1*], *Angela Candreva*[1], *Francesca Scarpelli*[1], *Alessandra Crispini*[1], *and Massimo La Deda*[1]
[1]*University of Calabria, Department of Chemistry and Chemical Technologies, Rende (CS), Italy,*
**giuseppe.dimaio@unical.it*

Keywords: Metal-enhanced fluorescence, Devices and Applications.

Assembly of gold nanoparticles in two-dimensional monolayers brings to new nanostructures with very interesting optical and electrical properties, opening the way to applications in optoelectronic and optothermal devices, sensors and so on. The self-assembly at water/hexane interface is one of the simplest and cheapest strategy to obtain highly ordered closed-packed gold nanoparticles monolayers [1]. Among the myriad of possible Au nanoparticles shapes, the cubic one having six planar facets and a strong plasmonic field localized on their sharp edges [2], are an ideal candidates as building blocks for the preparation of ordered 2D monolayers.

Gold nanocubes were synthesized by an optimized seed mediated growth approach [3], assembled in close-packed 2D array at water/hexane interface, using ethanol to destabilize the colloidal aqueous dispersion and 1-dodecanethiol to promote in-situ nanoparticles ordering [4,5], and then deposited on ITO or glass substrates using a modified drain-to-deposit approach [6]. The as-obtained macroscopic films (figure 1 a, b) characterized by UV-Vis spectroscopy, electronic microscopy (SEM), and X-Ray diffraction have shown promising properties for use both as metal-enhanced fluorescence substrates and as opto-thermal transducers.

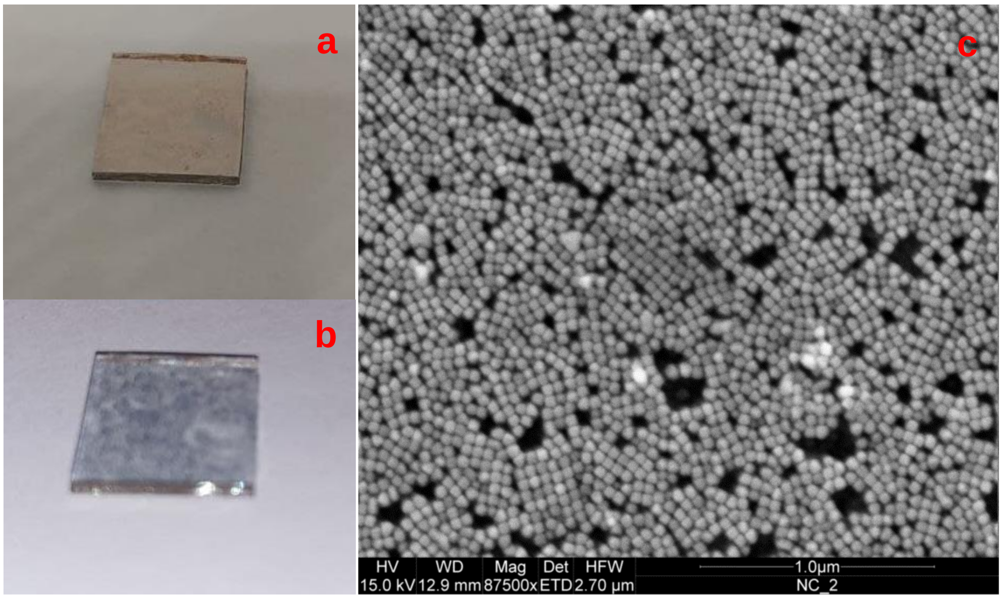

Figure 1: Optical image of a self-assembled monolayer of gold nanocubes deposited on ITO glass showing a gold coloration if observed in reflectance mode (a), and a dark blue coloration if observed in transmittance mode (b). Representative SEM image of a typical gold nanocubes self-assembled monolayer (c).

References

[1] Song L., Huang Y., Nie Z., Chen T., Nanoscale **12**, 7433-7460 (2020).

[2] Sturman B., Podivilov E., Gorkunov M., EPL **101**, 57009 (2013).

[3] Dovgolevsky E., Haick H., Small **11**, 2059-2066 (2008).

[4] Park, Y. K., Yoo, S. H. & Park, S. Langmuir **23**, 10505–10510 (2007).

[5] Park, Y. K. & Park, S. Chem. Mater. **20**, 2388–2393 (2008).

[6] Yang G., Hallinan Jr D. T., Nanotechnology **27**, 225604 (2016).

Microfabricated SiN membrane applied as a free-standing waveguide for refractive index sensing

Giulio Ferrando[1], Giacomo Manzato[1], Maria Caterina Giordano[1], Matteo Barelli[1], Debasree Chowdhury[1], Marco Centini[2], Francesco Buatier de Mongeot[1*]
[1]Dipartimento di Fisica, Università di Genova, Via Dodecaneso 33, I-16146 Genova, Italy
[2]Dipartimento di Scienze di Base ed Applicate per l'Ingegneria, Sapienza Università di Roma, Via Antonio

Functionalization of metasurfaces is gaining increasing interest for application in molecular and nanofluidic sensing [1-2]. In particular, the capability to engineer highly ordered arrays of antennas launching Rayleigh Anomalies (RAs), Localized Plasmon Resonance or guided modes represents a promising route to improve detection sensitivity, especially when the optical modes are tuned in resonance [3-4].
Here we demonstrate the versatile nanofabrication of a novel nanofluidic platform based on a free-standing Si_3N_4 membrane functionalized with plasmonic nanostripe gratings. Changing the pattern periodicity via high resolution electron beam lithography, is possible to introduce a shift of the photonic modes and the optical response of the array can be tuned across a broadband Visible and Near-Infrared spectrum. The high degree of control, provided by the top-down technique, allows to achieve precise tailoring of the nanogratings shape and periodicity, with an effective tuning of narrow-band optical modes which leads to the generation of guided modes in the supporting free-standing membrane thickness (200 nm). Moreover, with a proper geometry those guided modes interact with the broad plasmonic excitation of the nanostripes and exhibit an increased photonic response. Particular interest is thus dedicated to the creation of multiple patterns with different periods on a single free-standing membrane, leading to the observation of multiple, narrow absorption peaks corresponding to guided modes of different order. The spectral position of the guided modes is strongly influenced by the external surrounding medium, due to the evanescent behaviour of the field, therefore variations in refractive index at the interface can be detected tracking the spectral shift of such narrow guided modes [5]. Introducing different liquids in contact with the membrane, in consequence, one can observe a straightforward application of the system as a nanofluidic refractive index sensor with good RI sensitivity (180nm/RIU), measured collecting the transmitted signal in a simple optical microscopy configuration, competitive with respect to the state of art nanofluidic sensors. Perforation of the free-standing SiN membrane with arrays of nanoholes opens another route for functionalizing microfluidic devices with controlled mass flow in the active region of the membrane, where a modified photonic response is enabled by the plasmonic functionalization.

References

[1] M. C. Giordano et al., ACS Appl. Mater. Interfaces, 12, 9 (2020) 11155–11162
[2] M. Barelli et al., ACS Appl. Nano Mater., 3, 9 (2020) 8784–8793
[3] M. Bhatnagar, M. Gardella et al., ACS Appl. Mater. Interfaces, 13, 11 (2021) 13508–13516
[4] D. Chowdhury et al., J. Phys. Chem. C, 124 (2020) 17183−17190
[5] G.Manzato et al. Optics Express (2022) in press, https://doi.org/10.1364/OE.453135

A mid-infrared lab-on-a-chip for real-time reaction monitoring of liquids

Borislav Hinkov[1,*], Florian Pilat[1], Mauro David[1], Andreas Schwaighofer[2], Patricia L. Souza[1,3],
Benedikt Schwarz[1], Daniela Ristanic[1], E. Arigliani[1], Laurin Lux[2], Hermann Detz[1,4], Aaron M. Andrews[1],
Bernhard Lendl[2], and Gottfried Strasser[1]
[1]Institute of Solid State Electronics & Center for Micro- and Nanostructures, TU Wien, Vienna, Austria
[2]Institute of Chemical Technologies and Analytics, TU Wien, Vienna, Austria
[3]LabSem-CETUC, Pontifícia Universidade Católica do Rio des Janeiro, Rio de Janeiro, Brazil
[4]CEITEC, Brno University of Technology, Brno, Czech Republic
[*]borislav.hinkov@tuwien.ac.at

Keywords: Sensors and Biosensors, Spectroscopy and Nano-imaging, Devices and Applications

The mid-infrared (mid-IR) spectral range is highly suitable for selective and sensitive probing of molecules, by addressing their fundamental fingerprint absorptions. Liquids analysis in this wavelength range was long time limited to bulky detection systems like Fourier-Transform Interferometer (FTIR-)based sensors and liquid films on the order of a few micrometers only. This often resulted in time-consuming offline analytics. For this purpose, we present a novel monolithic high-performance mid-IR QC laser and detector (QCLD) device, enabling the next generation of liquid sensing. It is based on pioneering quantum cascade (QC) technology combined with novel mid-IR plasmonic concepts (Fig. 1(a)) [1–2]. The result is a monolithic, fingertip-sized optical sensor, highly suitable for liquid sensing [3]. In contrast to state-of-the-art systems, it allows real-time analysis of dynamical processes in liquids including inline and in-situ measurements. We demonstrate its breakthrough performance in analytical chemistry, through on-chip measurements of the time-dependent conformational changes of the model-protein bovine serum albumin (BSA, Fig. 1(b)) [3]. Time-resolved measurements are performed by combination with a custom-made 60-µl flow cell for inline measurements at $\lambda = 1620\ \mathrm{cm}^{-1}$ (Fig. 1(b)). We use a D_2O matrix for reduced background absorption, while maintaining comparable protein unfolding results as in biophysical buffer, i.e. H_2O. BSA unfolds irreversibly from α-helix to antiparallel β-sheets when heated from 20°C to 90°C (Fig. 1(b)). In our experiments we obtain the typical protein denaturation curves, following a sigmoidal Boltzmann equation (”s-shaped”) with increasing temperature (Fig. 1(c)). In good agreement with literature, we observe a decreasing transition temperature with increasing BSA-concentration [4]. By additionally directly submerging the sensor into a beaker with the protein-analyte and monitoring its absorbance vs concentration curve (calibration line), we can extract the important figures-of-merit of our on-chip detector. A comparison with a state-of-the-art attenuated total reflection (ATR-)FTIR reference system reveals the superior performance of our ultra-compact sensor with: 55-times higher absorbance, 120 times lower LOD ($\mathrm{LOD}_{\mathrm{QCLD}}$ ~75 ppm) and coverage of more than three order of concentrations of 0.0075 % to 9.23 %.

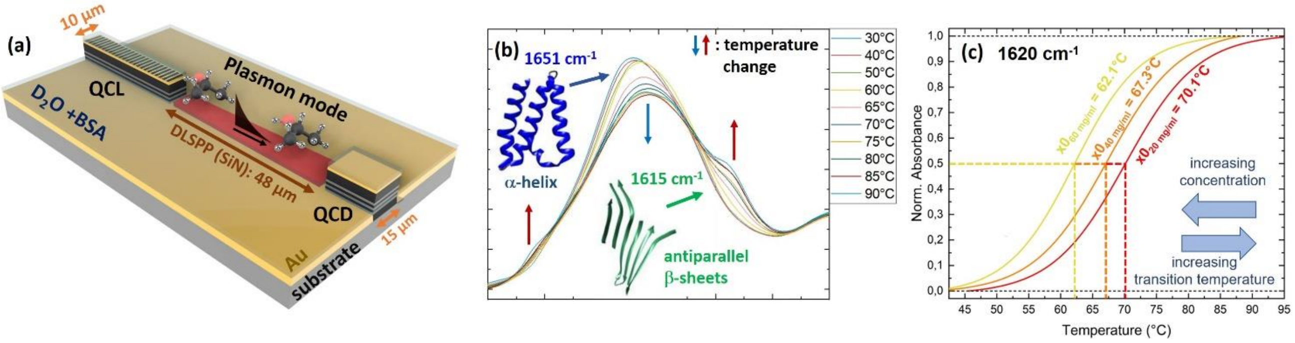

Figure 1: (a) Sketch of submerged QCLD-sensor (layers indicated). (b) Spectral changes during BSA denaturation process, when heating from 30°C to 90°C. (c) Normalized concentration-dependent denaturation curves (= sigmoidal Boltzmann fit to the experimental data), measured at λ~1620 cm^{-1} [4].

References

[1] B. Schwarz, P. Reininger, D. Ristanic, H. Detz, A. M. Andrews, W. Schrenk and G. Straßer, Nat. Commun. **5**, 4085 (2014).
[2] M. David, A. Dabrowska, M. Sistani, I. C. Doganlar, E. Hinkelmann, H. Detz, W. M. Weber, B. Lendl, G. Strasser and B. Hinkov, Opt. Express **29**, 26 (2021).
[3] B. Hinkov, M. David, F. Pilat, L. Lux, P. L Souza, A. Schwaighofer, B. Schwarz, H. Detz, A. M. Andrews, B. Lendl and G. Strasser, invited presentation at **10th** SciX conference (47th Federation of Analytical Chemistry & Spectroscopy Societies (FACSS) conference), Providence (Rhode Island), USA, 26th Sept, - 01. Oct. (2021).
[4] A. Schwaighofer, M. R. Alcaráz, C. Araman, H. Goicoechea and B. Lendl, Sci. Rep. **6**, 33556 (2016).

Mid-Infrared Nanospectroscopy of Misfolded Protein Aggregates

Antonia Intze[1,2], Maria Eleonora Temperini[1,2], Raffaella Polito[1], Elsa Zacco[3], Gian Gaetano Tartaglia[3], Annalisa Pastore[4], Michele Ortolani[1,2] and Valeria Giliberti[2]
[1] *Department of Physics, Sapienza University of Rome, Rome, Italy, antonia.intze@uniroma1.it*
[2] *Center for Life Nano- & Neuro-science, Istituto Italiano di Tecnologia (IIT), Rome, Italy*
[3] *Central RNA Laboratory, Istituto Italiano di Tecnologia (IIT), Genova, Italy*
[4] *The Wohl Institute at King's College London, London, United Kingdom*

Keywords: Spectroscopy and nano-imaging

Abstract - Photothermal expansion nanospectroscopy with a tunable quantum cascade laser is employed to study the morphology and quantify the secondary structure of subwavelength-size protein aggregates relevant for neurological diseases. Individual oligomers down to 100 nm diameter and 10 nm thickness are targeted at subsequent steps of the protein aggregation pathway.

Introduction - Protein aggregation is a common phenomenon in nature occurring both in physiological and pathological conditions. Self-assembly of proteins into oligomers within cerebral tissues has been linked with neurodegeneration, such as Alzheimer's disease [1]. Notwithstanding, the study of both morphology and secondary structure of these oligomers is challenging due to their transient nature and nanometer dimension [2]. The introduction of infrared (IR) nanospectroscopy techniques based on the use of high-resolution atomic force microscopy (AFM) led to a breakthrough in the study of proteins at the nanoscale. The sensitivity of IR nanospectroscopy is well beyond the light diffraction limit and as such enables to study the morphology and the secondary structure components (α-helix, β-sheet, turn, and random coil) of individual protein oligomers [3]. Here, we study the aggregation pathway of the transactive response DNA-binding protein 43 (TDP-43) by using the AFM-IR technique based on the photoexpansion effect (Fig. 1a). The aim is to target the structural heterogeneities among individual TDP-43 protein oligomers formed at different times.

Results - To obtain structural information as the aggregation proceeded, we deposited the TDP-43 protein oligomers on the gold surfaces at different times between 0 and 48 h (where t=0 h is the defrosting time). As a preliminary step, we performed a pure AFM topographic characterization of the samples (Fig. 1b). With the aim of characterizing the TDP-43 aggregation pathway, the AFM-IR spectra acquired on individual oligomers were fitted over the entire range (1450-1900 cm^{-1}). In the case of the Amide-I band related to C=O stretching mode of peptide bonds, we used five Lorentzian components centered at 1634, 1644, 1664, 1680, and 1690 cm^{-1}. Each Lorentzian component can be assigned to a different secondary structure component according to its frequency position (see inset of Fig. 1c). As TDP-43 protein aggregation continues, modifications with statistical significance are found in the Amide-I band indicating an increase of both parallel and anti-parallel β-sheet components, together with a decrease of the α-helix component (Fig. 1c).

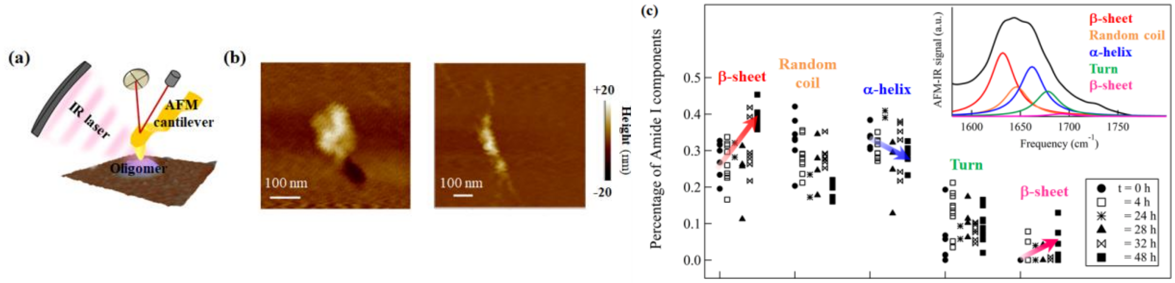

Figure 1: (a) Schematic depiction of the AFM-IR setup, (b) Representative AFM topography maps of isolated TDP-43 protein oligomers, (c) Trend of the percentage of Amide-I band components over aggregation time (0 to 48 h). Inset: Secondary structure deconvolution of Amide-I band related to one of the TDP-43 oligomers.

References

[1] E. Zacco, S.R. Martin, R. Thorogate, A. Pastore, *Frontiers in Molecular Neuroscience*, **11**, 1-11 (2018).
[2] J. Shenoy, N.E. Mammeri, A. Dutour et al., *The FEBS Journal*, **287**, 2449-2467 (2020).
[3] F.S. Ruggeri, G. Longo, S. Faggiano et al., Nat. Comun. **6**, 1-9 (2015).

Near-Unity Third-Harmonic Circular Dichroism in Silicon Chiral Metasurfaces

Yigong Luan[1], Luca Fagiani[2,3], Marco Gandolfi[4,5], Andrea Tognazzi[4,6], Kirill I. Okhlopkov[7], Attilio Zilli[1], Davide Rocco[5], Johann Osmond[3], Maxim R. Shcherbakov[7,8], Monica Bollani[2], Marco Finazzi[1], Costantino De Angelis[5], Michele Celebrano[1], Andrey A. Fedyanin[7] and Luca Carletti[5]

[1]*Department of Physics, Politecnico di Milano, Milano, Italy*
yigong.luan@polimi.it
[2]*CNR-IFN (Institute for Photonics and Nanotechnologies), LNESS laboratory, Como, Italy*
[3]*ICFO–Institut de Ciencies Fotoniques, The Barcelona Institute of Science and Technology, Barcelona, Spain*
[4]*CNR-INO (National Institute of Optics), Brescia, Italy*
[5]*Department of Information Engineering, University of Brescia, Brescia, Italy*
[6]*Department of Engineering, University of Palermo, Palermo, Italy*
[7]*Faculty of Physics, Lomonosov Moscow State University, Moscow, Russia*
[8]*Department of Electrical Engineering and Computer Science, University of California, Irvine, California, United States*

Polarization control through all-dielectric metasurfaces holds great potential in a wide variety of fields, such as quantum optical communications, biochemistry and holography. In particular, nonlinear metasurfaces yielding a high degree of circular dichroism, which indicates the degree to which these platforms couple to either left or right circularly polarized light, would enable the investigation of the chiro-optical properties of matter. This enables applications including chiral biosensing, polarization conversion, spin-controlled wave-front shaping, and chiral detectors. We have recently designed a silicon metasurface for third-harmonic generation (THG) featuring a high quality factor (Q). By performing back focal plane imaging, we observed a rich variety of linear polarization states of the nonlinear diffraction by the metasurface, thereby demonstrating the possibility of tailoring the polarization of the generated nonlinear diffraction orders [1]. Following a similar paradigm, by selecting resonances supported by specific meta-atoms geometries, the optimal coupling condition can be satisfied to achieve sizable enhancement of the circular dichroism [2]. We designed an asymmetric Si-embedded-in-SiO_2 metasurface featuring resonances with high Q and strongly selective response to the circular polarization state, resulting in a near-unity dichroism of the THG efficiency. Numerical simulations show that the nonlinear conversion factor (=THG power/cube of the pump power) of THG can reach values up to 10^{-2} W^{-2} by engineering Q ($>10^5$). This is obtained by optimizing the design of the metasurface to support quasi-bound states in the continuum, which also allows one to control both the linear and nonlinear circular dichroism [3]. Here we will show preliminary experimental results on a prototype of this metasurface fabricated according to the optimized parameters identified in [3]. To verify that the realized metasurface complies with the original design, we measured the transmission of both linearly and circularly polarized light in the linear regime. We first acquired linear polarization spectra identifying narrow polarization-selective resonances in the near infrared (NIR) (i.e. where the excitation for THG measurements will occur), which can be ascribed to high Q modes. We also performed circular dichroism measurements from the same metasurface in the linear regime. The observed dissymmetry factor for the circular polarization, although entangled with a large degree of linear dichroism that is always to be expected in such planar systems, is sufficiently large to be detected and shows spectral features in the NIR. After confirming these first results, we will address circular dichroism in the nonlinear regime.

References

[1] K. I. Okhlopkov, A. Zilli, A. Tognazzi, D. Rocco, L. Fagiani, E. Mafakheri, M. Bollani et al, Nano Lett. **21**, 10438 (2021).
[2] K. Koshelev, Y. Tang, Z. Hu, I. Kravchenko, G. Li, Y. Kivshar, arXiv:2202.12041 (2022).
[3] M. Gandolfi, A. Tognazzi, D. Rocco, C. D. Angelis, and L. Carletti, Phys. Rev. A **104**, 023524 (2021).

Electrical Modulation of the Optical Response of an Al-doped ZnO Thin Film

Riccardo Magrin Maffei[1,2], Alessandro di Bona[1], Maria Sygletou[3,4], Francesco Bisio[3,4], Sergio D'Addato[1,2],
Stefania Benedetti[1]
[1]*CNR-Istituto Nanoscienze, via G. Campi 213/a, 41125 Modena, Italy, riccardo.magrinmaffei@unimore.it*
[2]*Dipartimento di Scienze Fisiche, Informatiche e Matematiche, Università di Modena e Reggio Emilia,*
Via G. Campi 213/a, 41125 Modena, Italy
[3]*OptMatLab, Dipartimento di Fisica, Università di Genova, via Dodecaneso 33, 16146 Genova, Italy*
[4]*CNR-SPIN, C.so Perrone 24, 16152 Genova, Italy*

Al-doped Zinc Oxide (AZO) belongs to the family of Transparent Conductive Oxides (TCOs), which are a class of materials that displays a rare union of high optical transparency with high electrical conductivity. Their properties make them very interesting materials for optoelectronics, photovoltaics and infrared-plasmonic applications [1,2]. While the electrical and optical properties of this kind of materials can be widely tuned by modulating dopant concentration, a big challenge is their control by external excitation. A possible way is to exploit field effect by applying an external bias to an AZO thin film, and a proposed architecture for achieving that is a MOS capacitor [3]. The active medium is deposited on top of a $BaTiO_3$ (BTO) film, which is a high-κ dielectric and bestows a high capacitance to the system. Applying bias to the capacitor results in the creation of an accumulation or depletion zone at the interface between AZO and BTO, depending on the sign of the applied potential. This is expected to strongly change the dielectric permittivity of the AZO film near the interface with BTO [4,5].

The capacitors have been fabricated via Electron Beam Lithography (EBL) and their capacitance was measured by a precision impedance analyzer. They displayed a capacitance around 610-660 pF. The effect of charge injection/depletion in an epitaxial 30 nm thick AZO film deposited by magnetron sputtering has been investigated by means of in operando Spectroscopic Ellipsometry (SE) versus applied gate voltage. We have verified that an AZO epitaxial film displays far better electrical properties with respect to a polycrystalline one, and this improving is particularly pronounced at low thicknesses. We have observed a clear effect on the ellipsometric angles upon gating, that increases with applied voltage. According to preliminary calculations based on the Poisson equation, the accumulation/depletion zone width should be of the order of few nanometers, while the charge density variations should induce a change in the refractive index of around one. These changes will reflect on the shift in the crossover frequency and in the plasmonic response of the AZO film.

Figure 1: Proposed MOS capacitor architecture for gating of the AZO film.

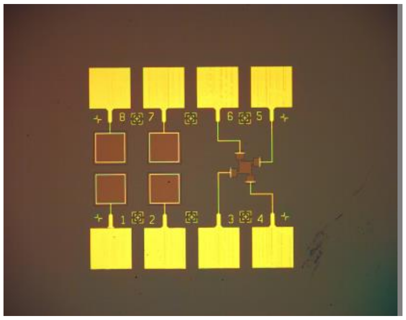

Figure 2: Four capacitors and one Hall probe fabricated via EBL.

References

[1] R. A. Afre, N. Sharma, M. Sharon and M. Sharon, Transparent Conducting Oxide films for various applications: a review, *Reviews on Advanced Materials Science* 53, 1, (2018)
[2] Y. Chen, Review of ZnO Transparent Conducting Oxides for solar applications, *2018 IOP Conf. Ser.: Mater. Sci. Eng.* 423 012170
[3] M. Sygletou, F. Bisio, S. Benedetti, P. Torelli, A. di Bona, A. Petrov and M. Canepa, Transparent conductive oxide-based architectures for the electrical modulation of the optical response: A spectroscopic ellipsometry study, *J. Vac. Sci. Technol. B* 37, 061209, (2019)
[4] E. Feigenbaum, K. Diest and H. A. Atwater, Unity-Order Index Change in Transparent Conducting Oxides at Visible Frequencies, *Nano Lett, 10*, 2111–2116 (2010)
[5] D. George et al., Electrically tunable diffraction efficiency from gratings in Al-doped ZnO, *Appl. Phys. Lett.* 110, 071110 (2017)

Magnetically co-doped Indium Tin Oxide nanoparticles (ITO-NPs) for magnetoplasmonic refractometric sensing

Ananthakrishnan Mohan[1], *Francesco Ciccarello*[1], *Alessio Gabbani*[1,2], *Francesco Pineider*[1]
[1] *University of Pisa, Pisa, Italy*
[2] *CNR-ICCOM, Sesto Fiorentino (FI), Italy*
ananthakrishnan.mohan@phd.unipi.it

Magnetoplasmonics is a subfield of active plasmonics where the Surface Plasmon Resonance is actively controlled by an external magnetic field.[1] Magneto-optical properties of plasmonic materials can be analysed and used in refractometric biosensing. The Localized Surface Plasmon Resonance (LSPR) present in gold nanoparticles (Au-NPs) was studied and the magnetic modulation amplitudes are found to be weak [2]. Indium Tin Oxide nanoparticles (ITO-NPs) exhibit LSPR in the NIR region and are optically transparent. Interestingly ITO-NPs show a strong magnetic modulation compared to Au-NPs since the effective mass of electron (m*) is lower than that in Au-NPs. Our group has assessed the superior magnetoplasmonic response of non-magnetic ITO NPs compared to metal-based NPs. [3]. For ITO-NPs it is possible to be co-doped with magnetic cations improving the magnetic modulation of LSPR provided that there is coupling between the magnetic cations and the charge carriers. The synthesis method employed is the thermal decomposition of organometallic precursors of Sn, In and the magnetic cations: Fe, Tb, Gd and Cr. The process was developed in our laboratory as a refinement of previously reported synthetic procedures [4]. Two series of co-doped ITO NPs (10% Sn) are compared: 5% and 2.5% of co-dopant. The sizes of particles are in the range 8-10 nm in all cases (Fig.1). LSPR properties of the samples were investigated by means of UV-Vis-IR spectrophotometry. We found that the Fe-ITO NPs present the lowest LSPR energy in both the series and it can be seen that Fe-doping has introduced a red shift in the LSPR energy in comparison with that of pristine 10% ITO-NPs. This could be result of the reduction of Fe (III) to Fe (II) absorbing free electrons, lowering the plasma frequency [5]. All other dopants introduce a blue shift in the LSPR with respect to the Pristine sample. The highest LSPR energy are those of Gd-ITO (2.5%) and Cr-ITO (5%). The Q factor of the LSPR signal, an important metric for potential application in refractometric biosensing follows the trend: Fe<Tb<Cr<Gd. Interestingly, the Q factor of Gd-ITO NPs is slightly higher than that of pristine ITO NPs. A paramagnetic nature is observed in the magnetometry analysis (Fig.2). Magnetic Circular Dichroism spectra (MCD) at room temperature were acquired using the 5% series. Fe-ITO NPs have the highest effective doping in both concentrations but broadening of the MCD signal is a disadvantage (Fig.3) The MCD results denote the possibilities of co-doping of Gd and Tb cations in ITO for better magnetic modulation. Low temperature MCD experiments are needed to study the magneto-optical nature of these particles to determine if magnetic coupling occurs between dopants and free carriers, which would result in a strong, temperature dependent magnetoplasmonic effect.

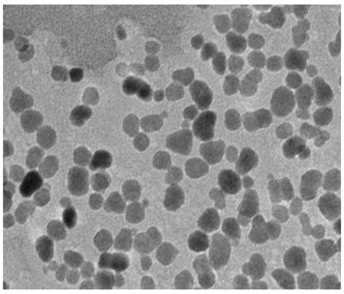

Fig.1: TEM image Gd-ITO 5%

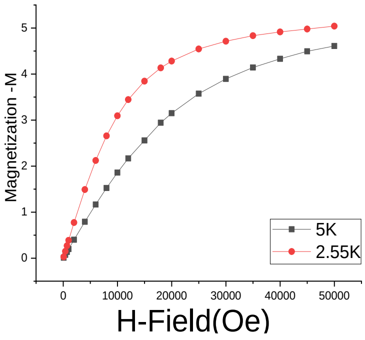

Fig.2: Magnetization curve (Gd-ITO at2.5K & 5K)

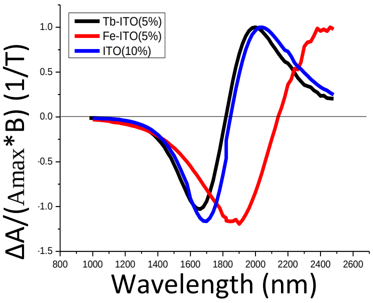

Fig.3: MCD spectra comparison of ITO, Fe-ITO & Tb-ITO

References:

1. Jiang, N., Zhuo, X., & Wang, J. (2017). Active plasmonics: Principles, structures, and applications. Chemical Reviews, 118(6)
2. Pineider, F., Campo, G., Bonanni, V., de Julián Fernández, C., Mattei, G., Caneschi, A., Gatteschi, D., & Sangregorio,C. (2013). Circular magnetoplasmonic modes in gold nanoparticles. Nano Letters, 13(10), 4785–4789.
3. Gabbani, Alessio et al. "Active Magnetoplasmonics with Transparent Conductive Oxide Nanocrystals." arXiv: Optics (2021)
4. Kanehara, M., Koike, H., Yoshinaga, T., & Teranishi, T. (2009). Indium Tin Oxide Nanoparticles with Compositionally Tuneable Surface Plasmon Resonance Frequencies in the Near-IR Region. Journal of the American Chemical Society, 131(49), 17736–17737.
5. Shanker, G. S., Tandon, B., Shibata, T., Chattopadhyay, S., & Nag, A. (2015). Doping controls plasmonics, electrical conductivity, and carrier-mediated magnetic coupling in Fe and Sn codoped in2O3 nanocrystals: Local structure is the key. Chemistry of Materials, 27(3), 892–900. https://doi.org/10.1021/cm5040936

Local optical properties of CVD-grown ML-WS_2 flakes on an ultra-dense plasmonic array of Au NPs

Lorenzo Ramò[1], Marzia Ferrera[1], Domenica Convertino[2,3], Giorgio Orlandini[2,3], Ilya Milekhin[4], Michele Magnozzi[1], Mahfujur Rahaman[4], Dietrich R.T. Zahn[4], Camilla Coletti[2,3], Maurizio Canepa[1] and Francesco Bisio[5].
[1]OptMatLab, Department of Physics, University of Genoa, Via Dodecaneso 33, 16146 Genoa, Italy,
[2] Center for Nanotechnology Innovation IIT@NEST, Piazza San Silvestro 12, 56127 Pisa, Italy
[3] Graphene Labs, Italian Institute of Technology, Via Morego 30, 16163 Genoa, Italy
[4] Institute of Physics, Chemnitz University of Technology, Reichenhainer Str. 70, 09107 Chemnitz, Germany
[5] CNR-SPIN, C.so Perrone 24, 16152 Genoa, Italy

ramo@fisica.unige.it

Keywords: Sensors and biosensors, plasmon-exciton polaritons, spectroscopy.

Two-dimensional transition metal dichalcogenides (TMDCs) can be coupled with plasmonic nanostructures in order to obtain new functionalities. In particular, Mo- and W-based sulphides and selenides possess optical properties ruled by excitons even at room temperature thanks to their high binding energies [1]. Since their atoms are almost exclusively on the surface, 2D TMDCs are very sensitive to their surrounding environment, but their extreme thinness weakens their light absorption. Plasmonic nanostructures are interesting because of their high optical absorption and their capability of manipulating and enhancing at the nanoscale the electromagnetic-field (EM). The integration of these two materials is a promising strategy to obtain heterostructures with a high interaction with light and a great sensitivity [2].

The system analysed is an heterostructure made of WS_2 flakes on top of a densely-packed array of gold nanoparticles (NPs). The optical response is measured as a function of the temperature, in the 75-350 K range, by means of variable-temperature micro-transmittance spectroscopies. What emerges is a weak interaction between the excitons of WS_2 and the localized surface plasmon resonance (LSPR) of the nanoparticles. The explanation we propose for this kind of interplay is the limited spillout of the electromagnetic field due to the close packing of the NPs array [3].

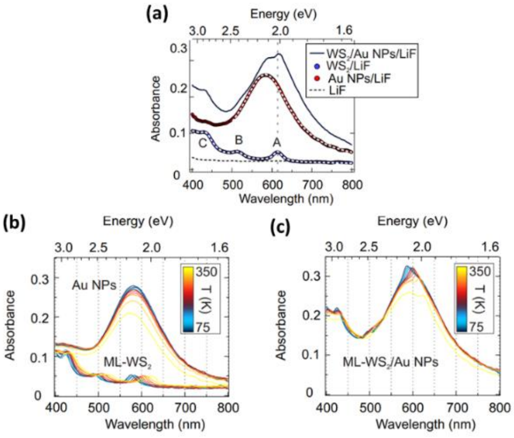

Figure 1: (a) Absorbance spectra of the hybrid systems and its components at room temperature; (b) Absorbance spectra as a function of the temperature of the plasmonic substrate and of ML-WS_2 without nanoparticles; (c) Absorbance spectra as a function of the temperature of the hybrid system made of ML-WS_2 and the array of Au NPs.

References

[1] Wang, G. and Chernikov, A. and Glazov, M. M. and Heinz, T. F. and Marie, X. and Amand, T. and Urbaszek, B. Colloquium: Excitons in atomically thin transition metal dichalcogenides. Rev. Mod. Phys. 2018, 90, 021001.
[2] Yan, S. and Zhu, X. and Dong, J. and Ding, Y. and Xiao, S. 2D materials integrated with metallic nanostructures: fundamentals and optoelectronic applications. Nanophotonics 2020, 9, 1877–1900
[3] Ferrera, M. et al. Optical Response of CVD-Grown ML-WS_2 Flakes on an Ultra-Dense Au NP Plasmonic Array. Chemosensors 2022, 10, 120

Raman scattering with near infrared excitation selectively resonant with the indirect bandgap of bulk $MoSe_2$

Simone Sotgiu[1], Tommaso Venanzi[1], Francesco Macheda[2], Elena Stellino[3], Paolo Postorino[1], Michele Ortolani[1] and Leonetta Baldassarre[1]
[1]*University of Rome, La Sapienza, Physics Department, 00185 Rome, Italy*
[2]*Istituto Italiano di Tecnologia, Graphene Labs, I-16163, Genoa, Italy*
[3]*Department of Physics and Geology, University of Perugia, via Alessandro Pascoli, Perugia, Italy*

Keywords: FT-Raman

Raman scattering is a powerful spectroscopic technique which enables the study of the vibrational and electronic excitations in solid-state systems. In particular, when the incoming laser energy matches a real electronic transition, i.e. resonance Raman scattering, the Raman process cross-section is strongly enhanced, leading to a higher visibility of otherwise hidden modes and of high-order Raman modes [1,2]. Here, we report Raman scattering with infrared excitation energy (1.16 eV) so to be in resonance with the indirect bandgap of bulk $MoSe_2$ (1.14 eV).

We have measured the Raman spectra (Figure 1a) of $MoSe_2$ in the visible (2.33 eV) and in the near-IR (1.16 eV). For the near-IR excitation energy we find a huge enhancement in the high-order Raman modes, together with a completely different lineshape, with respect to visible measurement (grey regions in Figure 1a). To confirm the resonant origin of these modes, we have evaluated the $MoSe_2$ phonon dispersion and, consequently, calculated the two-phonon density of states (2ph-DOS), i.e. the phonon DOS obtained as the sum of two phonons. We compare the 2ph-DOS evaluated along the entire Brillouin Zone (BZ) with the spectrum taken at 2.33 eV (Figure 1b, upper curves). The excellent agreement between the two curves allows us to assign at least the 580 cm^{-1} modes to sum of two phonons. We also compare the spectrum obtained with near-IR excitation energy with the 2ph-DOS restricted to the wavevector $\mathbf{q^*}$ of the indirect electronic transition between $\mathbf{\Gamma}$ and $\mathbf{T}$ points of the BZ (see Figure 1c). The qualitative agreement between the lineshapes and the relative weights of the peaks (see Figure 1b lower curves) are a clear indication that the 580 cm^{-1} modes originate from a resonance Raman process. We can thus assume that the resonant Raman process we are measuring is the following: an electron from the top of the valence band is excited and then scattered by a phonon with a wavevector $\mathbf{q^*} \approx \mathbf{T}$ which allows the transition to the conduction band minimum. Then, a second phonon with opposite wavevector $\mathbf{-q^*}$ brings the electron to the starting point of the BZ and it can relax radiatively emitting a photon (see Figure 1c).

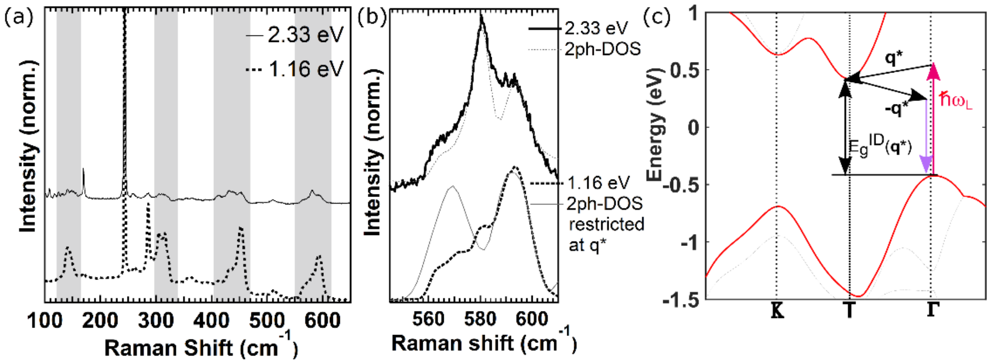

Figure 1: (a) Raman spectra measured on bulk $MoSe_2$ at different excitation energies, indicated in figure. (b) Zoom of the 580 cm^{-1} modes for 2.33 and 1.16 eV excitation energy, compared with DFT 2ph-DOS evaluated over the entire BZ (2.33 eV) and restricted to the phonons with wavevector $\mathbf{q^*}$ (1.16 eV). (c) Scheme of the resonant process.

As a future step we aim to couple layered semiconductor materials in their monolayer form with infrared plasmonic antennas. By exploiting the strong field enhancement provided in the antenna's hotsposts, we will be able to increase the Raman signal of the thin material, in a SERS-like experiment, using infrared excitation energies [3].

References

[1] Martin, R. M., and L. M. Falicov. *Light scattering in Solids I* (1983): 79-145.
[2] J. M. Calleja and M. Cardona. *Physical Review B*, vol. 16, no. 8, pp. 3753, 1977
[3] Giordano, Maria Caterina, et al. *ACS Applied Materials & Interfaces* 12.9 (2020): 11155-11162.

Infrared nanospectroscopy study of light-sensitive proteins with a plasmonic probe

Maria Eleonora Temperini[1, 2],Raffaella Polito[1],Leonetta Baldassarre[1],Michele Ortolani[1] and Valeria Giliberti[2]
[1] *Dipartimento di Fisica, Sapienza Università di Roma, Rome, Italy, mariaeleonora.temperini@uniroma1.it*
[2]*Istituto Italiano di Tecnologia, Center for Life Nano- & Neuro-Science, Rome, Italy*

Keywords: Spectroscopy and nano-imaging

Infrared (IR) spectroscopy in the mid-IR range (wavelength 5-20 μm) is broadly applied for the study of functional processes of biomolecules, as it can provide a label-free sensitivity to chemical bond orientation and length due to the specificity of vibrational fingerprints. However, the IR techniques are limited in terms of sensitivity and they require large quantities of molecules to probe, while preventing the possibility of investigating the intrinsic heterogeneity of the biological matter at the nanoscale. In the last years, various approaches have emerged to bring the IR spatial sensitivity at the nanometer size, taking advantage of plasmonic scanning probes. Here we present the photothermal-induced resonance (PTIR) method, also called AFM-IR, that couples the radiation emitted by a quantum cascade laser in the mid-IR range and a gold-coated tip of an atomic force microscope (AFM). The laser beam is focused on the AFM probe, which operates in contact mode with the sample. The laser emission wavelength is scanned in the IR range of interest (here 5 to 11 μm) and the thermal expansion generated by the local IR absorption results in a wavelength-dependent change of the indentation depth $\Delta\delta$ (Fig.1a) that is proportional to the IR absorption spectrum of the object under the AFM tip [1]. We apply the AFM-IR method to study two light-sensitive proteins, the Bacteriorhodopsin (BR) and the Channelrhodopsin-2 (ChR2). The latter are transmembrane proteins embedded in the lipid cell membrane that are involved in functional process of the host organism since they act, respectively, as proton pump and ion channel in response to the absorption of visible light at a specific wavelength. We investigate single membrane patches loaded with light-sensitive proteins and deposited on an ultraflat gold surface to exploit the plasmonic field enhancement in the nanogap between the gold-coated tip and the metallic surface (Fig.1b), reaching the sensitivity of monolayer samples (5 nm). The difference nanospectroscopy results we get are benchmarked with conventional micro-FTIR measurements and they display common features known to be related to the vibrational modes involved in the protein activity (Fig.1c) [2,3]. We conclude that the protein activity is preserved and measurable with our nanospectroscopy approach at the level of the single membrane patch.

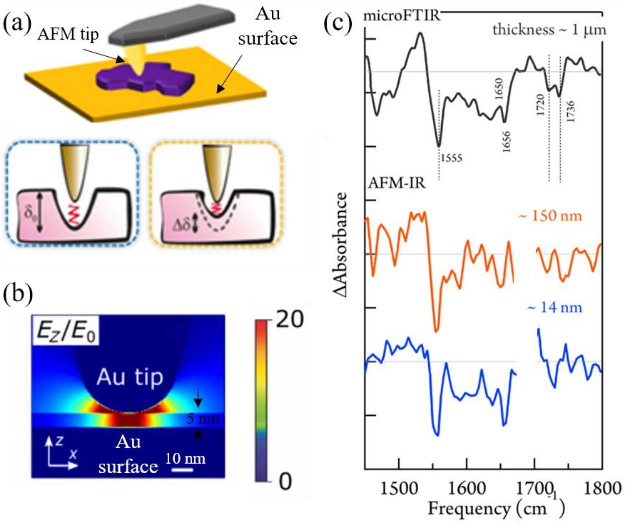

Figure 1: (a) Schematic sketch of AMF-IR technique. (b) Electromagnetic simulation of the IR radiation enhancement in the plasmonic nanogap. (c) Difference-absorbance results obtained on ChR2 sample with FTIR and AFM-IR measurements.

References

[1] A. Dazzi and C. B. Prater, Chem. Rev. **117**, 5146-5173 (2017).
[2] V. Giliberti et al. Nano Lett. **19**, 3104 (2019)
[3] R. Polito, M.E. Temperini et al. Phys. Rev. Applied **16**, 014048 (2021).

Light-triggered reversible deformations of a polymeric substrate in arbitrary directions

David Urban[1], Dag Roar Hjelme[1], Emiliano Descrovi[2],
[1]*NTNU, Trondheim, Norway, david.urban@ntnu.no*
[2]*Polito, Turin, Italy*

Keywords: Light-responsive polymers, Soft Microstructures,

Light-responsive polymers have in recent years attracted increasing attention due to their potential applications in areas such as fabrication of micro-structured surfaces, adaptive optics, and biology. For applications necessitating anisotropic deformations, sidechain azopolymers have been of particular interest, as some of them tend to deform along the axis of linear polarization of the incoming light. For example, directional deformation of azopolymer pillars on a glass substrate has been demonstrated to induce anisotropic behavior in attached living cells [1]. A major limitation of this type of microstructure is the limited reversibility of the induced plastic deformations. In a recent work carried out by Ryabchun et. al., the reversible deformation of azopolymer domains sparsely dispersed in a SEBS elastomer matrix was observed, reobtaining pristine domain shapes by heating or irradiation with circularly polarized light [2].

Here, we study the deformation and reversibility of a light-responsive substrate patterned with a hexagonal lattice of cylindrical pillars, prepared by dispersing azopolymers in SEBS at high concentrations (30 %wt.) and molding with a soft master. Figure 1a shows the displacement (magenta) resulting from the irradiation of the central area (yellow) with a horizontally linearly polarized CW green laser (561 nm, ~3W/cm^2) of a confocal microscope operating in continuous scanning mode. Enhanced contrast insets exemplify the local displacement of brighter spots, which extends also outside the directly irradiated region. An analysis in the Fourier space allows to estimate the shifts of the peaks related to the periodic pattern. In this way, the expansive and compressive strain along the polarization and the perpendicular directions can be quantified, (Figure 1b). Subsequently, the recovery of the initial shape after continuous scanning with circular polarization can be measured, allowing to quantitatively address in-plane expansion effects.

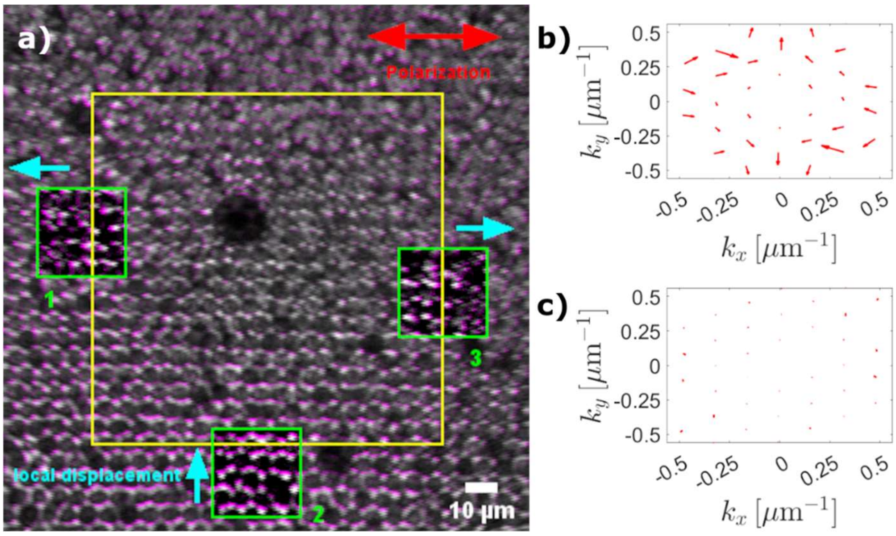

Figure 1: a) B/W: raw transmission image of substrate top surface with hexagonal pillar array. Magenta: pixels of raw transmission image after irradiation with horizontal polarization (initial image subtracted). Yellow: Zone of irradiation. Green: Enhanced contrast regions. b/c) Arrows showing displacement of peaks in Fourier space before and after irradiation with linear polarization (b) and before and after a complete cycle (linear + circular polarization) (c). Arrow magnification: x10.

In the future, we aim to explore the use of similar substrates for biological applications, where we believe that locally stretching zones through direct or indirect irradiation can be particularly advantageous.

References

[1] Puliafito, A. (2019). Driving Cells with Light-Controlled Topographies. *Advanced Science, 6*(14).
[2] Ryabchun, A. (2019). Photocontrollable Deformations of Polymer Particles in Elastic Matrix. *Advanced Optical Materials, 7*(24).

Plasmon-Induced Circular Dichroism of Gold Nanoparticles of Different Shapes

Rebecca Büchner[1], Jose Garcia-Guirado[1], Jaime Ortega Arroyo[1], and Romain Quidant[1]
[1]*Nanophotonic Systems Laboratory, Department of Mechanical and Process Engineering, ETH Zurich, 8092 Zurich, Switzerland*

Keywords: circular dichroism, chirality, plasmonic nanoparticles, chiroptical spectroscopy

Resonant plasmonic nanoparticles hold great promise in circular dichroism (CD) spectroscopy for enhancing the otherwise weak CD signals of molecules. In addition to enhancing the molecular CD signal, which is primarily in the UV range, the interaction of chiral molecules with achiral plasmonic particles can induce a CD signal at the resonance modes of the nanoparticles, which are typically in the visible-infrared range [1,2]. This effect, termed plasmon-induced CD, opens up new possibilities for detecting chiral molecules in the visible spectral range, thus allowing for the development of easier and more straightforward read-out approaches. However, the implementation of such plasmon-induced chiral samples remains poorly explored, as the strength of the induced CD signal is heavily affected by various factors, such as the spectral separation between the resonance of the nanoparticle and the chiral molecules, or the form and thickness of the molecular layer [3,4].

Here, we investigate the influence of nanoparticle shape on the plasmonic CD signal by comparing nanospheres, nanorods, and nanocubes functionalized with chiral ligands (Fig.1). We find that anisotropically shaped nanoparticles lead to a stronger plasmonic CD response than isotropically shaped ones. In particular, nanocubes exhibit larger CD values than nanospheres or nanorods, which we initially attribute to the presence of higher order modes on the edges of the cube. These results allow for a better choice of nanoparticles for plasmon-induced CD samples, and thus the development of more sensitive methods to detect molecular chirality in the visible spectral range.

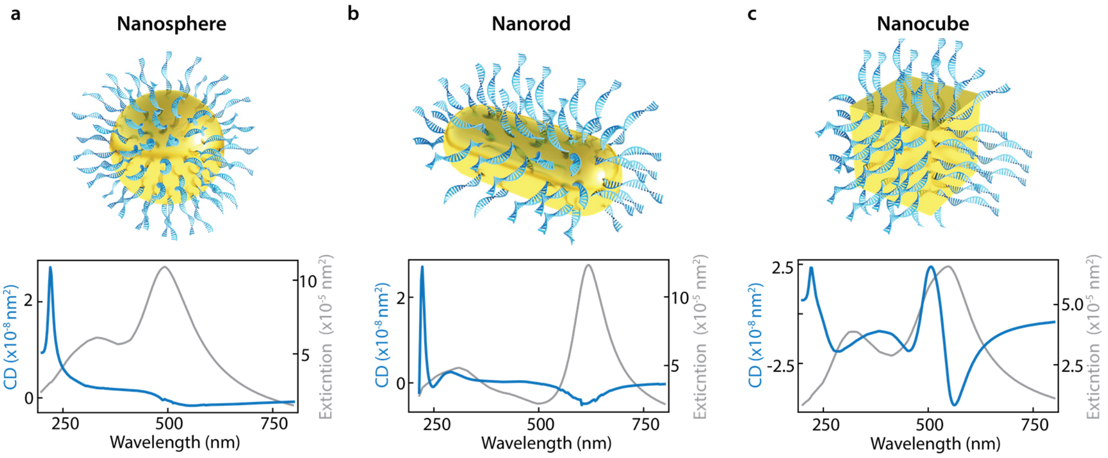

Figure 1: Plasmon-induced circular dichroism from a layer of chiral molecule covering gold nanoparticles of different shapes: (a) nanospheres, (b) nanorods, (c) nanocubes. Sketch of the gold nanoparticles coated with chiral molecules (upper row). Simulated CD and extinction cross-section spectra (lower row).

References

[1] A. O. Govorov, J. Phys. Chem. C 2011, 115, 16, 7914–7923
[2] J. M. Slocik et al., Nano Lett. 2011, 11, 2, 701–705
[3] B. M. Maoz et al., Nano Lett. 2013, 13, 1203−1209
[4] X. Lan et al., J.Am.Chem.Soc.2019, 141, 19336−19341

Determining the optical properties of Au nanorods using the metal nanoparticle boundary element method

The nanoscale morphology of metal nanostructures directly defines their optical, catalytic and electronic properties and even small morphological changes can cause significant property variations. With the development of single-particle (ultrafast) optical spectroscopy techniques and advanced electron microscopy these optical properties and morphology can be correlated on the single-particle level at the femtosecond temporal and atomic spatial scale, respectively. Electromagnetic simulations can play a key role in explaining the effect of these morphological differences on the optical properties of metal nanostructures. In this work, we used the metal nanoparticle boundary element method (MNPBEM) to deduce the optical properties of Au nanorods. The effect of parameters such as the discretization, dielectric function and substrate were studied. Finally, a comparison between an idealized model and electron tomography data confirmed the validity of our simulations.

Plasmon-driven Reactivity and Selectivity on Metal Nanoparticles Assessed by Quantum Chemical Simulations

Sadaf Ehtesabi[1], Siddhi Gojare[1], Zhandong Li[2], Dmitry Kurouski[2, 3], Stephan Kupfer[1], Stefanie Gräfe[1]
[1]*Institute of Physical Chemistry, Friedrich Schiller University, Jena, Germany, sadaf.ehtesabi@uni-jena.de*
[2]*Department of Biochemistry and Biophysics, Texas A&M University, College Station, Texas, United States*
[3]*Department of Biomedical Engineering, Texas A&M University, College Station, Texas, USA*

The control of chemical reactions by plasmon-driven catalytic processes is a highly active field in the chemical community. In this regard, the Kurouski group performed in-depth TERS studies of 2-nitro-5-thiolobenzoic acid (2-N-5TBA) surface-immobilized on either gold or palladium-coated gold nanoparticles (AuNPs and Au@PdNPs). Depending on the experimental setup, branching pathways yielding different products (and yields), e.g. various azo-species obtained upon dimerization. Therefore, a comprehensive understanding of the underlying mechanism is necessary to control the selectivity on the plasmon-driven reaction.

We aim at modeling the chemical interaction of a plasmonic gold and palladium surface with 2-N-5TBA. In this way, we study how plasmonic-hybrid systems behave and how plasmons cause different reactions that result in product variations. The driving forces for various pathways and the directionality of light-driven charge transfer allowed us to elucidate the production braching at a quantum mechanical level.

Density functional theory (DFT) as implemented in the GPAW code [1] with the ASE interface was used. The optB88-vdW functional is employed on a real space grid. The Au and Pd slab is represented by 4x4x3 Au(111) and Pd(111) surfaces resulting in 3 layers of 16 metal atoms with two-dimensional periodic boundary conditions. Furthermore, the electronic nature of photo-processes in resonance upon 633-nm photoexcitation (1.96 eV) of the plasmonic-hybrid system(s) were investigated at the non-periodic time-dependent DFT (TDDFT) level of theory using the Gaussian 16 program [2]. In particular, the photoinduced redox chemistry between the metal cluster (Au or Pd) and the respective substrate (educt, intermediate, product state) were assessed. The electronic character, i.e. local excitation of the substrate as well as charge transfer excitation between the substrate and the metal cluster, was evaluated based on charge density differences (CDDs).

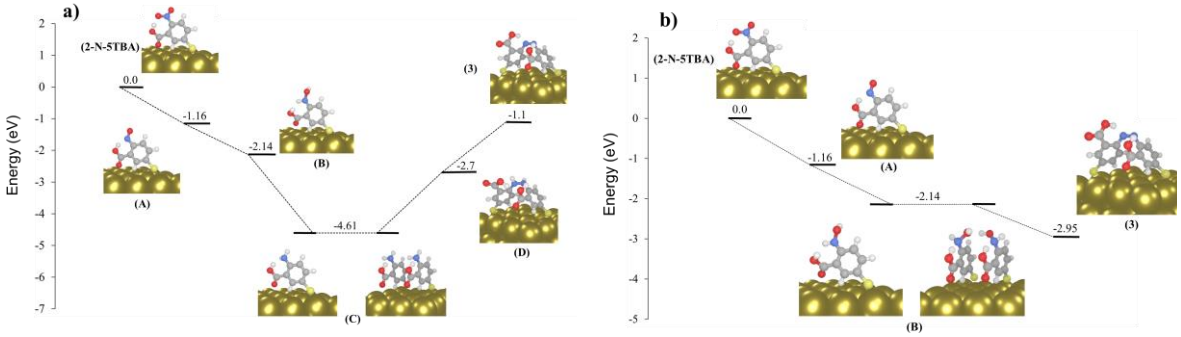

Figure 1: 2-N-5TBA dimerizes to bi-carboxyl-DMAB through a series of redox reactions, forming different intermediates.

References

[1] J. Enkovaara, C. Rostgaard, J. J. Mortensen, et. al., J. Phys.: Condens. Matter **22**, 253202 (2010).
[2] M. J. Frisch, G. W. Trucks, H. B. Schlegel, et. al., Gaussian 16, Gaussian, Inc., Wallingford CT, 2016.

Bottom-up and top-down synthesis of Au@AZO core@shell nanomaterials

Quynh Nguyen[1], *Attilio Zilli*[2], *Agostino di Francescantonio*[2], *Michele Celebrano*[2], *Andrea Baldi*[1]
[1]*Vrije Universiteit Amsterdam, Amsterdam, the Netherlands, q.nguyen@vu.nl*
[2]*Politecnico di Milano, Milan, Italy*

Aluminium doped zinc oxide (AZO) is a cost-efficient, highly earth-abundant, conductive, transparent and chemically-, mechanically- but most importantly photo-stable material which additionally exhibits non-linear optical phenomena such as third- and second harmonic generation. These properties make it an attractive material for photocatalysis, optoelectronic devices and nanolasers [1].

Plasmonic systems such as gold nanoparticles (Au NPs) can amplify the optical response of a photonic material as the localised surface plasmon resonances (LSPRs) strongly enhance the near-field. This phenomenon is for example taken advantage of in photo-detectors with an increase in their photo-sensitivity [2].

In this project we develop the synthesis of Au@AZO core@shell nanomaterials using both a bottom-up colloidal method and a top-down single-particle approach.

The colloidal synthesis is based on a modified hydrothermal procedure used to prepare Au@ZnO nanoparticles [3]. The top-down approach, exploits the plasmonic photothermal heating of a gold nanoparticle under focused laser irradiation while being immersed in an aqueous AZO precursor solution. We follow the shell formation by monitoring the increase in the scattering cross-section of the nanoparticles and a red-shift in their resonance wavelength [4].

Our approach has the potential to generate hybrid plasmonic nanostructures with controlled levels of aluminum doping and tailored shell thicknesses for opto-electronic applications.

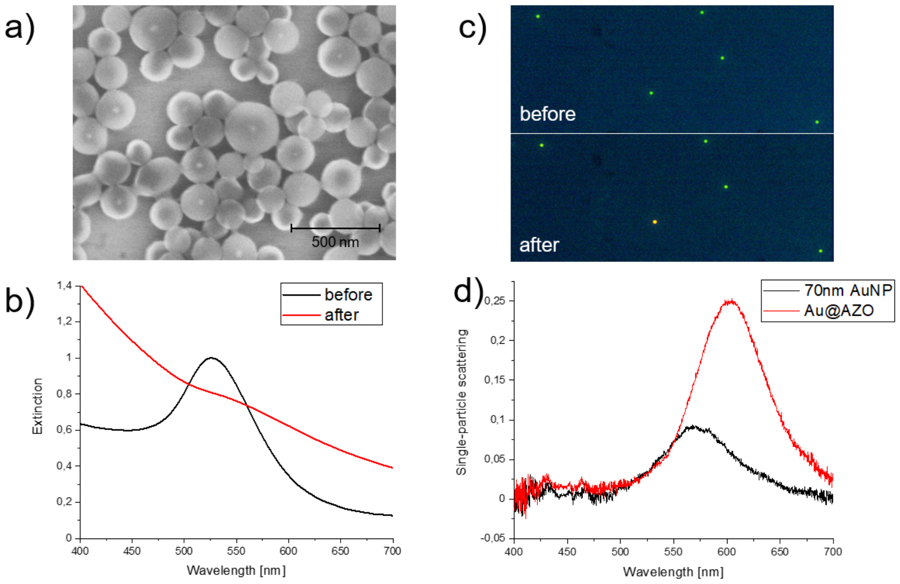

Figure 1: a) Scanning electron microscope image of Au@AZO core@shell nanoparticles obtained by colloidal hydrothermal synthesis. b) UV-Vis spectrum of colloidal Au@AZO reaction solution before and after hydrothermal synthesis. c) Dark-field microscope image of 70 nm Au nanoparticles before and after illumination with a 532 nm laser. d) Single-particle scattering spectra of a 70 nm AuNP before and after AZO shell growth.

References

[1] F. Maldonado and A. Stashans, “Al-doped zno: Electronic, electrical and structural properties,” *Journal of Physics and Chemistry of Solids*, vol. 71, no. 5, pp. 784–787, 2010.

[2] A. Dorodnyy, Y. Salamin, P. Ma, J. V. Plestina, N. Lassaline, D. Mikulik, P. Romero-Gomez, A. F. i Morral, and J. Leuthold, “Plasmonic photodetectors,” *IEEE Journal of Selected Topics in Quantum Electronics*, vol. 24, no. 6, pp. 1–13, 2018.

[3] Y. Yang, S. Han, G. Zhou, L. Zhang, X. Li, C. Zou, and S. Huang, “Ascorbic-acid-assisted growth of high quality m@ zno: a growth mechanism and kinetics study,” *Nanoscale*, vol. 5, no. 23, pp. 11808–11819, 2013.

[4] R. Kamarudheen, G. Kumari, and A. Baldi, “Plasmon-driven synthesis of individual metal@ semiconductor core@ shell nanoparticles,” *Nature communications*, vol. 11, no. 1, pp. 1–10, 2020.

Thermo-optical bistability in single semiconductor super-cavity

Daniil Ryabov[1], Olesia Pashina[1], George Zograf[1], Sergey Makarov[1], Mihail Petrov[1]
[1]School of Physics and Engineering, ITMO University, St. Petersburg, Russia, 197101
daniil.ryabov@metalab.ifmo.ru

Optical heating of resonant nanostructures is an important feature in semiconductor nanophotonics which depending on application could have either positive or negative effect on device operation. Although linear heating regime has been extensively studied for both plasmonic and all-dielectric resonators, there is still no rigorous approach to estimate high-intensity light irradiation of semiconductor particles. In this work we are focusing on describing the systems which intrinsic material properties change under laser beam excitation because of temperature increase. We develop simple analytical model for this problem and provide numerical simulation for nonlinear heating of nanoparticle supporting quasi bound in continuum state mode (quasi-BIC or so-called 'super-cavity mode'). Efficient light-to-heat conversion in such nonlinear systems is accompanied with thermo-optical bistability which could find applications in all-optical sensors, detectors and opto-electronic devices.

Analytical model of optical heating is based on the coupled mode equation [1] for a single resonator which allows to calculate stored energy inside of the nanostructure by knowing its eigenmode parameters. If the complex refractive index depends on temperature and, hence, on the field amplitude, then eigenfrequency and losses rate should be modified and equation becomes self-consistent. This results into three possible states and hysteresis-like response of the system (Fig. 1b). By analyzing temperature dependence of the resonator on pump intensity and laser detuning from the eigenfrequency position one could obtain width W_h and height H_h of the hysteresis area and also reveal the nonlinear critical coupling condition. In contrary to classical linear case this condition implies counterintuitive spectral mismatch between laser and 'cold' resonator frequency necessary to achieve maximal heating efficiency (Fig. 1c).

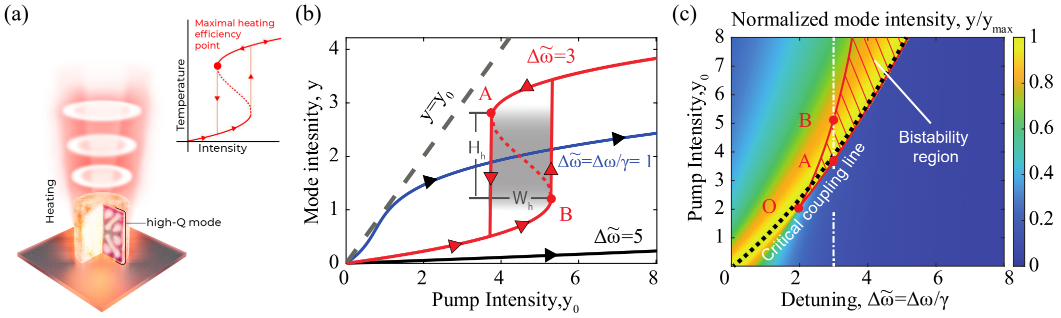

Figure 1: Bistability in single nanoresonator. a) Schematic view of super-cavity excitation by cylindrical vector beam. b) Mode intensity as a function of pump intensity. Red curve indicates hysteresis-like thermal response of the system. c) Mode intensity map as a function of laser detuning and pump intensity. Black dashed line depicts critical coupling condition in nonlinear system [2].

Since light-to-heat conversion efficiency strongly depends on resonator quality factor, we search for quasi-BIC eigenmode in silicon nanocylinder so as to suppress radiative losses of the system [3]. Nonradiative losses are compensated by doping the structure and increasing imaginary part of refractive index according to Drude model [4]. The nanoparticle is then irradiated with azimuthally polarized vector beam and resulting temperature is evaluated (Fig. 1a). Numerical simulations also provide us with hysteresis response of the output temperature which is in perfect coincidence with the results of analytical model. Bistability regime appears at relatively low incident intensity around 1 mW/μm^2 and, therefore, discovered phenomenon is perspective for various nanophotonic applications. Moreover, we believe that developed approach is quite universal and could be applied to other types of nonlinearity.

References

[1] Haus, H. Waves and fields in optoelectronics. PRENTICE-HALL, INC., ENGLEWOOD CLIFFS, NJ 07632, USA, 402 (1984).
[2] Ryabov, D., Pashina, O., Zograf, G., Makarov, S. and Petrov, M. Nonlinear optical heating of all-dielectric super-cavity: efficient light-to-heat conversion through giant thermorefractive bistability. Nanophotonics (2022).
[3] Koshelev, K., et al. Subwavelength dielectric resonators for nonlinear nanophotonics. Science 367.6475 (2020): 288-292.
[4] Ryabov, D., Pashina, O., Zograf, G., Makarov, S. and Petrov, M. Optical heating of doped semiconductor nanocylinders supporting quasi-BIC modes. Journal of Physics: Conference Series. Vol. 2015. No. 1. IOP Publishing (2021).

Charge transfer in hybrid metal-semiconductor systems at a single NP level and correlation to morphology

Francesca Scalerandi[1], *Mees Dieperink* [1], *Wiebke Albrecht* [1]
[1]*Department of Sustainable Energy Materials, AMOLF; Science Park 104, 1098 XG 10 Amsterdam, The Netherlands*

Noble metal plasmon nanoparticles (NPs) exhibit unique optical properties arising from the local surface plasmon resonance (LSPR) effect. These properties make them very attractive for many applications, such us sensing, catalysis and solar cells. However, the life time of electron-hole pairs in metal plamsonic NPs is ultrashort[1], resulting in very low charge separation efficiencies. A solution that has been widely explored is to hybridize plasmonic NPs (donors) with semiconductors (acceptors). At the interface the Fermi levels are aligned and the so called Schottky barrier is formed. The hot electrons are injected in the semiconductor by means of different mechanisms resulting in a dramatic reduction of charge recombination in the metal. In this project we want to dive into the charge transfer mechanism. The redistribution of the hot carriers strongly depends on the quality and electronic nature of the interface. By fine tuning the semiconductor (QDs) energy levels, the Schottky barrier can be controlled to achieve the optimal trade off between forward and back electron transfer.

In this project we aim to investigate and possibly quantify charge transfer efficiency at a single particle level. Optical properties, obtained through dark field scattering (DFS) and photoluminescence (PL) and performed in a single particle optical set up, are correlated to the exact morphology investigated by electron tomography on the exact same single hybrid nanosystem. The final goal is to correlate optical properties to exact morphology and tune the latter to achieve the optimal efficiency of charge transfer. First optical measurements of charge transfer have been carried out for two gold nanorods (AuNRs) separated by short distances, as shown in Figure 1. The two NRs have been brought in closed vicinity by exchange the CTAB for a Benzene-1 4-dithiol (BDT). This molecule has a quite high conductivity ($10^6 S/m$), allowing charge transfer to happen by means of hopping for bigger distances compared to vacuum.

Regarding hybrid nanostructures, AuNR-ZnS have been chosen as first system. First attempt to electrochemically grow ZnS[2] only in the hot spot of the plasmonic NPs by making use of the hot electron created in the hotspot upon plasmon decay[3] have been carried out.

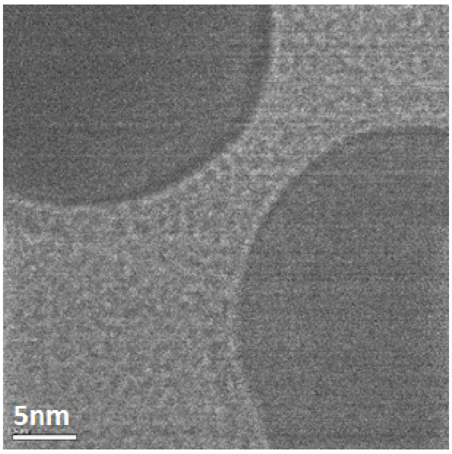

Figure 1: TEM images of AuNRs dimers after ligand exchange with BDT

References

References

[1] K. Wu, J. Chen, J. R. McBride and T. Lian, *Science*, 2015, **349**, 628–632.
[2] H. Wang, W. Zhao, C. H. Xu, H. Y. Chen and J. J. Xu, *Chemical Science*, 2019, **10**, 9308–9314.
[3] E. Kontoleta, A. Tsoukala, S. H. Askes, E. Zoethout, E. Oksenberg, H. Agrawal and E. C. Garnett, *ACS Applied Materials and Interfaces*, 2020, **12**, 35986–35994.

Shaping ZnO nanoparticles: Effect of nanoparticle morphology on caffeine degradation

*S. Thakur[1, 2], S. Neogi[1] and A. K. Ray[3]
[1] Indian Institute of Technology Kharagpur, India, [2] Politecnico di Torino, Italy [3] University of Western Ontario, Canada
*shaila.thakur@hotmail.com

Caffeine is a common micropollutant and one of the most abundant xenobiotics due to its high daily consumption across the globe. The use of caffeine is not only limited to food industries, but it is also extensively used in the pharmaceutical industry. Studies report that when mussels were exposed to caffeine concentrations usually found in water samples, they stopped producing a protein that protects their DNA, exposing them to a risk of genetic mutation [1]. Researchers also indicated the presence of caffeine in the tissue of fishes and other marine organisms. Thus, it is imperative to ensure that the water discharged into the rivers and oceans have been treated for caffeine removal.

Most of the traditional methods for the treatment of wastewater are easy to handle and reusable [2]. However, various commonly used techniques such as activated sludge, ion-exchange and coagulation have low treatment efficiencies and they are not cost effective in the long run. Even the advanced techniques such as membrane filtration faces a serious drawback of fouling that increases energy consumption and lowers the separation efficiency. To overcome these obstacles, we have developed a method for the activation of ZnO nanoparticles using solar light. This method significantly reduces the operating costs as solar light is inexpensive compared to the UV light. We engineer nanoparticle shapes to achieve the best photocatalytc activity at a low ost. To the best of our knowledge, this is the first report to study the comparative solvent induced morphology-dependent photocatalytic mechanism of action of ZnO nanostructures.

In this study, we obtained different shapes of ZnO nanoparticles by varying the type of solvent used [3]. We could tune the amount of reactive oxygen species (ROS) and metal ion (Zn^{2+}) generation from nanostructures, which in turn dictates their activity. ZnO nanostructures were fabricated via facile wet chemical method by varying the type of solvents. From the SEM images (Figure 1a–c), ZnO appears as well-defined nanospheres, nanorods and nanopetals under the influence of different solvents. PEG400 gives rise to spherical morphology; for water, we obtain petals attached to each other and for toluene, we obtain nanorod like structure.

From the TEM images (Figure 1d–f), nanospherical ZnO are the smallest of all structures with an average diameter of 10.18 nm. Nanorods exhibited a mean width of 157 nm and a length of 1.43 µm while nanopetals have an average thickness of 31.85 nm. The ROS and Zn^{2+} ions generated by these nanostructures were mainly responsible for the nanoparticle activity. The ROS consisted of O^{2-} and OH● while H_2O_2 was found to be insufficient to show any photocatalytic activity. The morphological parameters are listed in Table 1.

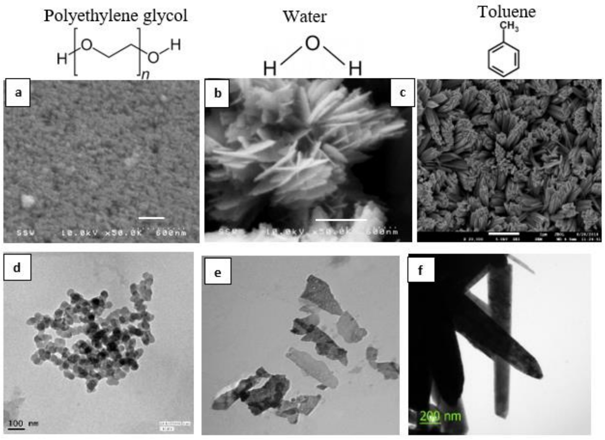

Fig. 1. SEM (a-c) and TEM (d-f) images of ZnO nanomaterials synthesized in different solvents (a) PEG400 (b) water (c) toluene [3]

Table I: Characterization of ZnO nanostructures [3]

Sample	Average Particle diameter (nm) (TEM)	BET specific surface area (m^2/g)	Total pore volume (cc/g)	Average pore diameter (nm)	Point of zero charge
Sphere	10.18	92.22	0.15	6.64	4.90
Petal	31.85 (petal thickness)	12.02	0.03	10.70	6.00
Rod	157.00 nm (diameter)	6.60	0.01	10.26	6.80

After the adsorption equilibrium was reached, the samples were exposed to 250mW/cm^2 of simulated solar light and 1.0 g/L nanoparticle dosage for the photocatalytic experiments. The photocatalytic data was fitted to pseudo-first order and pseudo-second order kinetic model, as shown in Figure 2. It was seen that the experimental data can be suitably represented by both the kinetic models with high correlation coefficients. The rate constants for ZnO sphere falls with the rise in amount of caffeine. ZnO spheres exhibited the highest value of degradation rate constant at the lowest caffeine concertation of 10 ppm (k_1-1.323min^{-1}, k_2-1.74 g/mg min). This is about 1.1

times (k_1 and k_2) higher than that achieved by petals whereas 1.6-(k_1) and 2.2-(k_2) times higher than the degradation achieved by ZnO rods. At highest concentration, ZnO spheres are 1.4-(k_1) and 2.8-fold (k_2) higher than ZnO petals whereas 2.6-(k_1) and 2.5-fold (k_2) higher compared to ZnO rods.

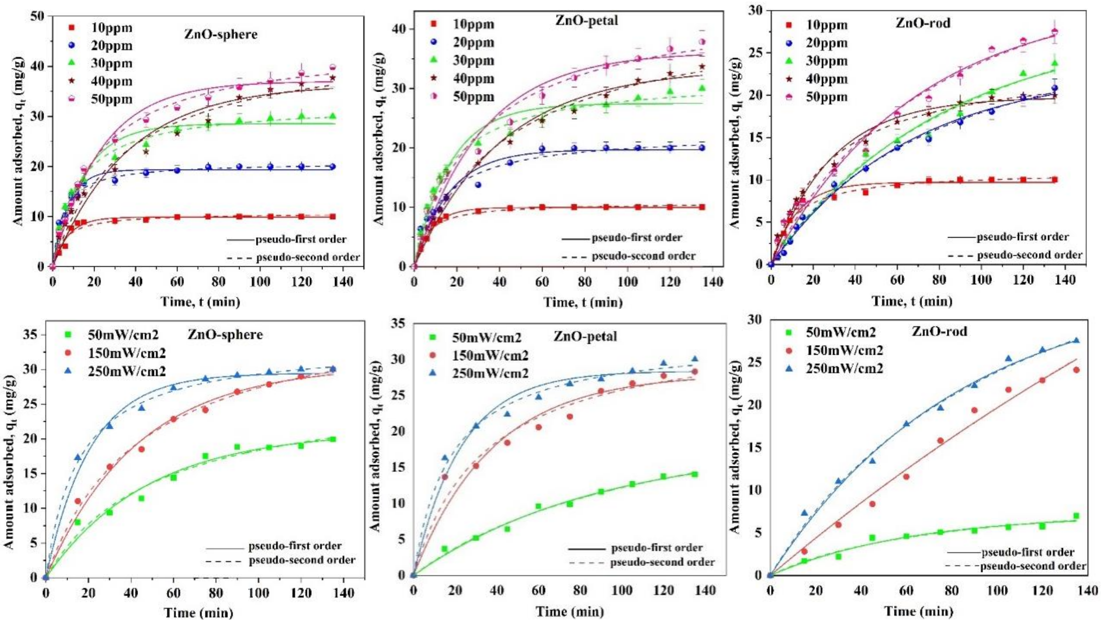

Fig. 2. Kinetic model for the adsorption of caffeine on ZnO nanostructures at (a–c) various caffeine concentrations and (d–f) different light intensity. (—) and (- - -) represent pseudo-first-order and pseudo-second-order models, respectively [3]

Thus, we see that there is a correlation between the shape of nanoparticles and their photocatalytic activity. While this is a specific case of effect of nanoparticle shape on caffeine degradation, yet the theory that nanoparticle morphology affects its activity can be extended to almost all applications of nanoparticles known till date.

References: 1) Rodriguez del Rey, Zoe, "Occurrence and Concentrations of Caffeine in Seawater from the Oregon Coast and Potential Effects on the Dominant Mussel, Mytilus californianus" (2010). Dissertations and Theses. Paper 722. https://doi.org/10.15760/etd.722

2) Rajasulochana, P.; Preethy, V. Comparison on efficiency of various techniques in treatment of waste and sewage water—A comprehensive review. Resour. Effic. Technol. 2016, 2, 175.

3) Thakur, S.; Neogi, S.; Ray, A.K. Morphology-Controlled Synthesis of ZnO Nanostructures for Caffeine Degradation and *Escherichia coli* Inactivation in Water. Catalysts 2021, 11, 63.

Nonlinear optical sensing in arrays of plasmonic nanoparticles

Augustin Verneuil[1, 2], Attilio Zilli[2], Christian Jonin[3], Andrea Locatelli[4], Marco Finazzi[2],
Michele Celebrano[2] and Anne-Laure Baudrion[1]
[1]*Light, Nanomaterials, Nanotechnologies, Université de Technologie de Troyes, 12 rue Marie Curie, 10004 Troyes, France. Email: augustin.verneuil@utt.fr*
[2]*Dipartimento di Fisica, Politecnico di Milano, Piazza Leonardo da Vinci 32, 20133 Milano, Italy*
[3]*Institut Lumière Matière, Université Claude Bernard Lyon 1, Bâtiment Alfred Kastler, 10 Rue Ada Byron, 69622 Villeurbanne, France*
[4]*Dipartimento di Ingegneria dell'Informazione, Università degli Studi di Brescia, via Branze 38, 25123 Brescia, Italy*

Keywords: Nonlinear plasmonics, Metamaterials, Sensors and Biosensors

Second-harmonic generation (SHG) from metallic nanoparticles (MNPs) is a promising strategy for optical sensing. Indeed, in centrosymmetric materials SHG mostly originates from the breaking of symmetry at the interface, providing a sensitive way to probe surface effects. In MNPs, SHG can additionally be enhanced by plasmonic effects, with the best improvements being obtained in structures supporting resonances at both the fundamental and harmonic wavelengths. [1]

Owing to these properties, biosensing devices based on these properties have been proposed in several works in the recent years, e.g. mercury in water and blood [2] or single molecules of rhodamine 6G [3]. In particular, Ghirardini et al. [4] showed that an array of such multiply resonant particles (fig. 1a), could achieve significantly better figures of merit at the SH compared to the fundamental wavelength (fig. 1b), despite a very low SH absolute yield. In this previous study, the main limiting factor was the cancellation of SH signal in the far field, due to the subwavelength pitch of the array that only allowed the 0th diffracted order.

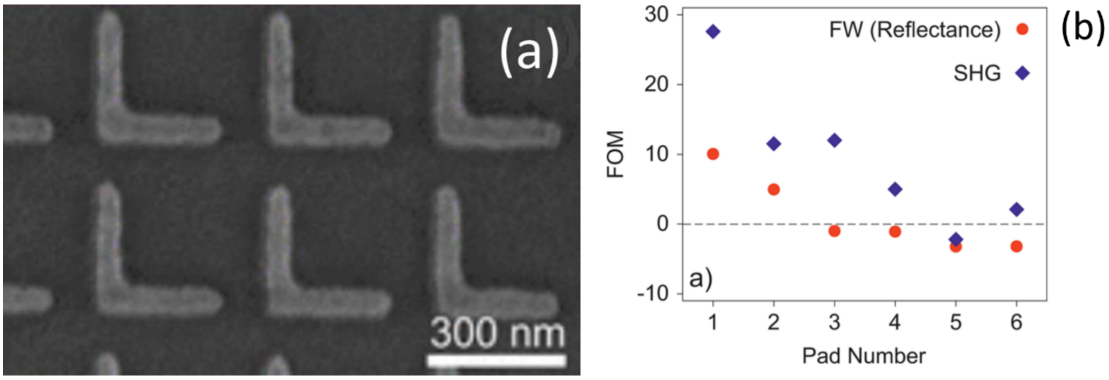

Figure 1: (a) Scanning electron microscopy image of the L-shaped particles studied in [4], supporting orthogonally-polarized plasmonic resonances at the fundamental and harmonic wavelength. (b) Figure of merit (FOM, calculated as $(\Delta I/I_{ref})/\Delta n$, where I and I_{ref} are the intensity of reflected/emitted light from the pad of interest and its corresponding reference, respectively) of the array response at both the pump and SH wavelength, each pad corresponding to a different particle size (135 to 285 nm). All figures reproduced from [4].

Our strategy to improve the performance of this platform is then to attune the emission pattern of the individual particles with the collective response of the array. In this work, we started by numerically calculating the far-field SH radiation pattern of a single antenna, before optimizing the pitch of the array to improve the SH extraction.

References

[1] Celebrano, M., Wu, X., Baselli, M., Großmann, S., Biagioni, P., Locatelli, A., De Angelis, C., Cerullo, G., Osellame, R., Hecht, B., Duò, L., Ciccacci, F., & Finazzi, M. Nature Nanotechnology, *10*, 412-417 (2015).
[2] Verma, M. S., & Chandra, M. ACS Sensors, *5*, 645-649 (2020).
[3] Sahu, S. P., Mahigir, A., Chidester, B., Veronis, G., & Gartia, M. R. Nano Letters, *19*, 6192-6202 (2019).
[4] Ghirardini, L., Baudrion, A.-L., Monticelli, M., Petti, D., Biagioni, P., Duò, L., Pellegrini, G., Adam, P.-M., Finazzi, M., & Celebrano, M. Journal of Physical Chemistry C, *122*, 11475-11481 (2018).

Actively tunable hybrid-2D angle-sensing photodetectors

Tom Hoekstra[1], *Jorik van de Groep*[1]
[1]*Van der Waals-Zeeman Institute, University of Amsterdam, Amsterdam, The Netherlands, t.hoekstra@uva.nl*

Photodetectors are semiconductor-based devices that convert absorbed photons into electrical signals and thereby measure the information carried by light. Conventional bulk photodetectors are limited by the materials' properties and require additional filters and optical elements to retrieve multi-dimensional components including color, polarization, and incidence angle. To this end, resonant semiconductor nanostructures are a promising platform to tailor a detector's spectral responsivity and polarization sensitivity, without the need for external filters [1]. Moreover, optical coupling of the resonant modes can be designed to facilitate angle-dependent absorption and scattering [2]. However, utilizing such geometrical resonances for actively tunable devices proves challenging, because these are fixed in the fabrication stage and offer only weak electrical tunability.

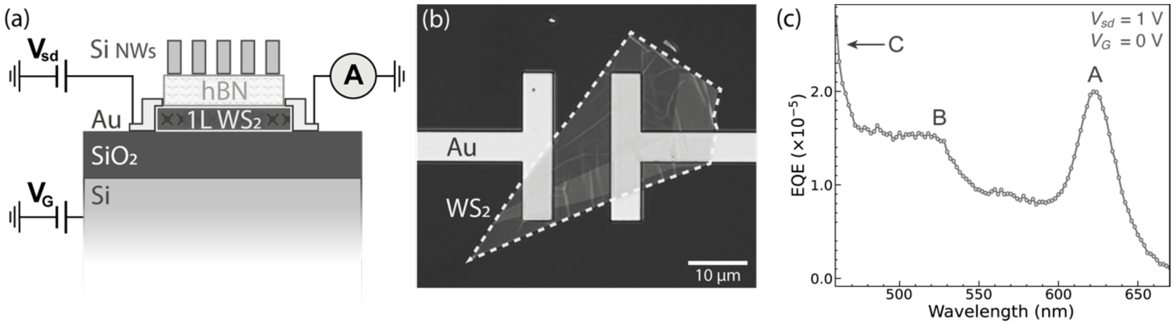

Figure 1: ***(a)*** *Schematic of a monolayer (1L) WS_2 photodetector functionalized with Si nanowires (NWs) for angle-selective detection. Photocurrent is extracted from the WS_2 channel with the applied source-drain voltage (V_{sd}), while the detection angle is modulated by the gate bias (V_G).* ***(b)*** *Few-layer WS_2 photodetector prototype.* ***(c)*** *The photodetector's external quantum efficiency (EQE) probes absorption and is dominated by the exciton resonances (A, B, C).*

Here, we leverage geometry-independent exciton resonances in atomically thin WS_2 to realize actively tunable angle sensors. The photodetector is comprised of Au electrodes and monolayer WS_2 in a metal-semiconductor-metal geometry, capped by a thin layer of insulating hBN to prevent degradation of the monolayer's optoelectronic properties due to fabrication and environmental adsorbates (Fig. 1a). To this end, we use a deterministic dry-transfer technique to assemble devices from tape-exfoliated WS_2 and hBN flakes. The first prototype consists of few-layer WS_2 transferred onto an oxidized Si substrate with prepatterned electrodes fabricated by e-beam lithography (Fig. 1b). Under illumination, photocurrent is extracted from the WS_2 channel by the applied source-drain voltage (V_{sd}) and is modulated with the gate voltage (V_G). The device's external quantum efficiency spectrum clearly probes absorption in the nanolayer and without gating it is dominated by the excitons (Fig. 1c).

Angle sensing is accomplished by functionalizing the photodetector with a high quality-factor, non-local metasurface. We design a subwavelength grating comprised of Si nanowires with the period and fill-factor tailored to control leaky modes guided along the surface. At the detection angle, free-space light can couple to the structure's quasi-guided mode by matching of the in-plane wave vector. The mode profile is designed to overlap with the WS_2 A-exciton and thus drastically enhance light absorption at resonance. Electrical gating alters the exciton resonance and this changes the mode index, thereby allowing active variation of the detection angle. These results pave the way for the development of next-generation, highly compact and tunable photodetectors.

References

[1] Q. Li, J. van de Groep, Y. Wang, P. Kik & M. Brongersma, Nature Communications **10**, 4982 (2019).
[2] S. Yi *et al.,* Nature Nanotechnology **13**, 1143-1147 (2018).